

Renormalization group study of superfluid phase transition: Effect of compressibility

Michal Dančo*

*Institute of Experimental Physics SAS, Watsonova 47, 040 01 Košice, Slovakia*Michal Hnatič[†]*Institute of Experimental Physics SAS, Watsonova 47, 040 01 Košice, Slovakia;
Bogolyubov Laboratory of Theoretical Physics, Joint Institute for Nuclear Research, 141980 Dubna, Russian Federation;
and Faculty of Science, Šafárik University, Moyzesova 16, 040 01 Košice, Slovakia*Tomáš Lučivjanský[‡]*Faculty of Science, Šafárik University, Moyzesova 16, 040 01 Košice, Slovakia*Lukáš Mižišin[§]*Institute of Experimental Physics SAS, Watsonova 47, 040 01 Košice, Slovakia
and Bogolyubov Laboratory of Theoretical Physics, Joint Institute for Nuclear Research, 141980 Dubna, Russian Federation*

(Received 17 October 2019; revised 24 June 2020; accepted 22 July 2020; published 14 August 2020)

Dynamic critical behavior in superfluid systems is considered in the presence of external stirring and advecting processes. The latter are generated by means of the Gaussian random velocity ensemble with white-noise character in time variable and self-similar spatial dependence. The main focus of this work is to analyze an effect of compressible modes on the critical behavior. The model is formulated through stochastic Langevin equations, which are then recast into the Janssen-De Dominicis response formalism. Employing the field-theoretic perturbative renormalization group method we analyze large-scale properties of the model. Explicit calculations are performed to the leading one-loop approximation in the double (ε, γ) expansion scheme, where ε is a deviation from the upper critical dimension $d_c = 4$ and γ describes a scaling property of the velocity ensemble. Altogether five distinct universality classes are expected to be macroscopically observable. In contrast to the incompressible case, we find that compressibility leads to an enhancement and stabilization of nontrivial asymptotic regimes.

DOI: [10.1103/PhysRevE.102.022118](https://doi.org/10.1103/PhysRevE.102.022118)**I. INTRODUCTION**

Scaling behavior and related concepts arguably provide many fruitful views, not only in theoretical physics [1,2]. Though initially scaling came to prominence in the field of high energy physics and critical phenomena, nowadays, many of its applications can be found in such diverse research areas as biology [3,4], finance [5], population dynamics [1,6], epidemics spreading [7], and others.

Among the most studied systems in physics, exhibiting scaling behavior, is superfluid phase transition in liquid helium. In this paper we are concerned with a specific aspect of critical dynamics in the vicinity of the λ point in superfluid helium ^4He . In the seminal review of Hohenberg-Halperin [8], these authors categorized various dynamical models to which renormalization group methods have been applied. In order to categorize other forms as well they have denoted these models in alphabetical order so that E designates a symmetric planar magnet, while F designates an asymmetric

planar magnet. In the more general model F, dynamics is captured by three fields. Two of them, ψ and ψ^\dagger , correspond to order parameters and stand for expectation values of the microscopic bosonic operators $\hat{\psi}$ and $\hat{\psi}^\dagger$. The third field m describes temperature fluctuations in a system. Interactions between fields are determined from the generalized Poisson brackets, whose forms follow from physically motivated considerations [1,9]. Model E can be interpreted as a simplified version of model F in which a certain temperature dependence has been neglected [9,10] and physically different variables are employed. However, in practical terms this amounts to the appearance of a complex kinetic coefficient and an intermode cubic coupling term [9,10]. Both models E and F have been analyzed predominantly by renormalization group (RG) methods [1,9–11]. There remains a longstanding issue [1,9,12–14] related to determination, which fixed point of the RG flow actually corresponds to a macroscopically observable regime in experiments. This is not only an academic problem as ensuing nonasymptotic effects hinder experimentally measurable quantities. Possible solutions involve (i) the search for correct microscopic model for superfluidity [14,15], (ii) elaborating existing numerical results through multiloop calculations [16–19], or (iii) appropriate generalizations of models [13,14].

In this work, we follow option (iii) by means of inclusion of external velocity fluctuations into the model description. In

*michal.danco@gmail.com

†hnatic@saske.sk

‡tomas.lucivjansky@upjs.sk

§mizisin@theor.jinr.ru

this regard several generalizations have already been proposed [13,20,21]. It has been shown that incompressible hydrodynamic fluctuations contribute significantly to the value of the ω_w index, which controls the stability of large-scale regimes [9,17]. This index is related to a RG behavior of a ratio of two kinetic coefficients (in this paper the corresponding ratio is related to a parameter u introduced later in Sec. II).

However, the overall conclusions are by no means decisive. The main problem we want to address in this paper is to analyze the presence of solenoidal modes in velocity fluctuations. In particular, we study what effects in comparison with the incompressible case can be expected and to what extent critical behavior is affected.

Similarly to typical advective problems in fluid dynamics [22–24] we incorporate the velocity fluctuation field \mathbf{v} by substituting the partial time derivative ∂_t with a convective derivative of the form $\partial_t + (\mathbf{v} \cdot \nabla)$. From general considerations [25], we expect that the presence of external disturbance, e.g., random impurities or turbulent mixing, might lead to completely new types of critical behavior with richer and more exotic properties [26–29].

To fully specify a theoretical setup let us briefly describe the employed model for velocity fluctuations. We assume that the velocity $\mathbf{v} = \mathbf{v}(t, \mathbf{x})$ is a random stochastic Gaussian variable with prescribed statistical properties [24,30]. In the original formulation [31], the velocity field was further taken to be isotropic, incompressible, and decorrelated in a time variable. Without loss of generality, we can set the mean value $\langle \mathbf{v} \rangle = 0$ and take the pair velocity function in the following form:

$$\langle v_i v_j \rangle \propto \delta(t - t') k^{-d-y} T_{ij}, \quad (1)$$

where k is the wave number, $0 < y < 2$ is a free parameter with the realistic (“Kolmogorov”) value $y = 4/3$, d is a space dimension, and tensor T_{ij} carries information about the vectorial character of velocity modes. This model attracted a lot of interest in the past mainly because of insights it offers into the origin of intermittency and the anomalous scaling in the fully developed turbulence [24,30]. Naively, basic premises of such models might be perceived as too crude and unrealistic. Nevertheless, important effects of parity breaking, anisotropy, or compressibility are easily taken into account [30,32–35]. It turns out that then the phenomenon of intermittency is even more pronounced than in genuine turbulent flow. Recent studies have also pointed out some significant differences between the zero and finite correlation time problems [34,36,37] and between the compressible and incompressible cases [38,39].

Let us point out a crucial difference between critical dynamical models and the model considered in this work. The basic assumption of the former models is the presence of ambient thermal fluctuations. Coupling with a thermal bath provides the necessary means by which a critical steady state can be maintained. Deviations from thermal equilibrium are considered small that result in a variety of relations between different physical quantities [11]. A well-known example is the fluctuation-dissipation theorem, which relates a two-point correlation function to susceptibility [1,10]. On the other hand, inclusion of external velocity fluctuations effectively drives the critical system away from the thermal equilibrium and leads to an effectively nonequilibrium system. Hence, re-

lations like the fluctuation-dissipation theorem cease to hold, and as a consequence, a theoretical analysis becomes more involved.

In relation to this paper, there was recently put forward an intriguing approach to a similar problem. In contrast to the standard approach to critical systems, in which dynamical models are constructed using generalized Poisson brackets or symmetry considerations [9], a particular microscopic approach was suggested [14,40,41]. The authors have analyzed various aspects of phase transitions in superfluids by means of a nontrivial technique that uses nonequilibrium Green’s functions [42]. In particular, an implicit assumption common to many critical models related to the incompressibility of underlying fluid [43] was put into question. Relaxing this condition with the allowance of compressible modes results in an effective model fully equivalent to model A of critical dynamics [8]. This result seems peculiar as model A is conceivably the simplest dynamical extension of the well-known φ^4 model [10,44]. The one-component order parameter takes the simple form

$$\mathcal{S}_A = - \int d^d x \left(\frac{1}{2} (\nabla \varphi)^2 + \frac{\tau}{2} \varphi^2 + \frac{g}{4!} \varphi^4 \right), \quad (2)$$

also known in the literature as Landau-Ginzburg-Wilson action functional [1,10,44]. As experiments are still lacking in this direction, suggested models are still waiting for a decisive affirmation of their relevance for critical dynamics.

The paper is organized as follows. In Sec. II we give a formulation of the problem by means of Langevin equations. These are then rewritten into the field-theoretic model using the Janssen–De Dominicis formalism. The resulting action is amenable to the field-theoretic renormalization group analysis, which is carried out in Sec. III. Section IV is devoted to a detailed analysis of fixed points’ structure, and Sec. V is reserved for a calculation of experimentally relevant critical exponents. Concluding remarks are summarized in Sec. VI. Appendixes A, B, and C contain technical details about divergent parts of Feynman diagrams, lengthy expressions of RG functions, and coordinates of fixed points.

II. FIELD-THEORETICAL FORMULATION

Using the standard terminology proposed in Ref. [8], model E of critical dynamics is described by the nonconserved two-component order parameter composed of two (complex) conjugated fields, $\psi(t, \mathbf{x})$ and $\psi^\dagger(t, \mathbf{x})$, and a conserved scalar field, $m(t, \mathbf{x})$. The former can be viewed as macroscopic averages of the Bose-particle field operators, whereas the latter field $m(t, \mathbf{x})$ is a certain linear combination of energy and mass density [10] (or a normal component of the magnetization in antiferromagnetic materials). Time evolution of the fields is governed [1,9,10] by the following set of equations:

$$\partial_t \psi = \lambda_0 \frac{\delta \mathcal{S}_{st}}{\delta \psi^\dagger} + i\lambda_0 g_{30} \psi \frac{\delta \mathcal{S}_{st}}{\delta m} + f_\psi, \quad (3)$$

$$\partial_t \psi^\dagger = \lambda_0 \frac{\delta \mathcal{S}_{st}}{\delta \psi} - i\lambda_0 g_{30} \psi^\dagger \frac{\delta \mathcal{S}_{st}}{\delta m} + f_{\psi^\dagger}, \quad (4)$$

$$\partial_t m = -\lambda_0 u_0 \nabla^2 \left(\frac{\delta \mathcal{S}_{st}}{\delta m} \right) + i\lambda_0 g_{30} \left(\psi^\dagger \frac{\delta \mathcal{S}_{st}}{\delta \psi^\dagger} - \psi \frac{\delta \mathcal{S}_{st}}{\delta \psi} \right) + f_m, \quad (5)$$

where $\nabla^2 = \sum_{i=1}^d \partial^2 / \partial x_i \partial x_i$ is the Laplace operator in d -dimensional space, $\partial_t = \partial / \partial t$ is the time derivative, and λ_0 is a kinetic coefficient related to diffusive modes. Let us note that, when necessary, we write space dimension d explicitly. This is due to a later use of the RG approach. In contrast to action (2), now the static action functional \mathcal{S}_{st} is given by the following form in the critical region:

$$\mathcal{S}_{\text{st}} = \int d^d x \left(\psi^\dagger \nabla^2 \psi - \frac{1}{2} m^2 + m h_0 - \frac{1}{6} g_{10} (\psi^\dagger \psi)^2 \right), \quad (6)$$

and the substitution $\varphi(\mathbf{x}) \rightarrow \varphi(t, \mathbf{x})$ is implicitly assumed in Eqs. (3)–(5) in terms stemming from variational derivatives for any member from the set $\varphi \in \{\psi, \psi^\dagger, m\}$. Parameters g_{10} and g_{30} play the role of the coupling constants of the theory [1,10]. Random forces f_ψ , f_{ψ^\dagger} , and f_m are assumed to be Gaussian random variables with zero means and correlators D_ψ , D_{ψ^\dagger} , and D_m with the white noise character in a time variable. In the time-momentum representation they are given by the following formulas:

$$D_{\psi^\dagger}(p, t, t') = D_\psi(p, t, t') = \lambda_0 \delta(t - t'), \quad (7)$$

$$D_m(p, t, t') = \lambda_0 u_0 p^2 \delta(t - t'). \quad (8)$$

Parameter u_0 is dimensionless and has been introduced for future convenience. Here and below, the bare (unrenormalized) parameters in the renormalization group sense are denoted with the subscript 0. The normalization in relations (7) and (8) has been chosen in such a way that the steady-state equal-time correlation functions of the stochastic problem are calculable exactly with the Boltzmann factor $\exp(\mathcal{S}_{\text{st}})$. The stochastic problem, Eqs. (3)–(5), (7), and (8), can be concisely reformulated by means of the Janssen–De Dominicis functional formalism [45,46]. The ensuing field-theoretic action of model E [1,9,10] then directly follows:

$$\begin{aligned} \mathcal{S}_E = & 2\lambda_0 \psi^\dagger \psi' - \lambda_0 u_0 m' \nabla^2 m' + \psi^\dagger \{ -\partial_t \psi + \lambda_0 [\nabla^2 \psi \\ & - g_{10} (\psi^\dagger \psi) \psi / 3] + i\lambda_0 g_{30} \psi [-m + h] \} + \text{H.c.} \\ & + m' \{ -\partial_t m - \lambda_0 u_0 \nabla^2 [-m + h] \\ & + i\lambda_0 g_{30} [\psi^\dagger \nabla^2 \psi - \psi \nabla^2 \psi^\dagger] \}. \end{aligned} \quad (9)$$

The abbreviation H.c. stands for a Hermitian conjugate part of the action with respect to the ψ field. In action (9) we have employed a condensed notation, in which integrals over space-time are implicitly included. For instance, the second term in Eq. (9) is an abbreviated form of the expression $m' \partial^2 m' = \int dt \int d^d x m'(t, \mathbf{x}) \nabla^2 m'(t, \mathbf{x})$. Prime fields ψ' and $\psi^{\dagger'}$ correspond to auxiliary Martin-Siggia-Rose response fields [47]. A functional formulation effectively means that the statistical averages of the random quantities in the original stochastic problem, Eqs. (3)–(5), can be represented by functional integrals over the full set of fields with the weight functional $\exp(\mathcal{S}_E)$. In quantum-field-theory terminology various correlation functions then correspond to Green's functions of the field-theoretic model with action (9). Such a formulation is especially convenient for the further use of field-theoretical methods such as the Feynman diagrammatic technique and perturbative renormalization groups, which provide the main theoretical tools in this work.

The next step consists of an introduction of the velocity fluctuations into a theoretical model. According to a standard approach [23,30,43], it is sufficient to replace the partial time derivative ∂_t by the Lagrangian derivative $\partial_t + (\mathbf{v} \cdot \nabla)$. However, in the presence of compressibility this is not sufficient [48], and the following substitutions are necessary:

$$\partial_t \psi \rightarrow \partial_t \psi + (\mathbf{v} \cdot \nabla) \psi + a_{10} \psi (\nabla \cdot \mathbf{v}), \quad (10)$$

$$\partial_t m \rightarrow \partial_t m + (\mathbf{v} \cdot \nabla) m + a_{20} m (\nabla \cdot \mathbf{v}). \quad (11)$$

Without the inclusion of terms proportional to parameters a_{10} and a_{20} , the model ceases to be multiplicatively renormalizable.

In this work we employ the Kraichnan rapid-change model [30,31,39] with compressibility of the fluid taken into account. Accordingly, the velocity field \mathbf{v} is assumed to be a random Gaussian variable with prescribed statistical properties. By a proper substitution we can always achieve that $\langle \mathbf{v} \rangle = 0$. Due to the Gaussian character of \mathbf{v} , the only needed information lies in a specification of the two-point correlation function, which assumes the following form:

$$\langle v_i(t, \mathbf{x}) v_j(t', \mathbf{x}') \rangle = \delta(t - t') D_{ij}(\mathbf{x} - \mathbf{x}'), \quad (12)$$

where the Dirac delta function ensures the Galilean invariance of the model [23]. Due to the translational invariance of the flow, it is convenient [30] to specify the kernel function D_{ij} in Eq. (12) in the Fourier representation

$$D_{ij}(\mathbf{r}) = D_0 \int \frac{d^d k}{(2\pi)^d} \frac{\theta(k - l_v)}{k^{d+y}} [P_{ij}(\mathbf{k}) + \alpha Q_{ij}(\mathbf{k})] e^{i\mathbf{k} \cdot \mathbf{r}}, \quad (13)$$

where $P_{ij}(\mathbf{k}) = \delta_{ij} - k_i k_j / k^2$ and $Q_{ij}(\mathbf{k}) = k_i k_j / k^2$ are the transverse projector and the longitudinal projector, respectively. Further, $k = |\mathbf{k}|$ is the wave number, $D_0 > 0$ is an amplitude factor, and $\alpha \geq 0$ is an arbitrary parameter, which might be interpreted as a degree of compressibility in the system [34,49]. The Heaviside function $\theta(x)$ ensures infrared (IR) cutoff of the theory that does not violate Galilean invariance. The momentum IR scale l_v is related to the external scale of velocity fluctuations L crudely as $l_v \sim 1/L$, but the precise form is unimportant for the later discussion.

The case $\alpha = 0$ corresponds to the incompressible fluid ($\nabla \cdot \mathbf{v} = 0$), whereas $\alpha > 0$ describes a deviation from the incompressibility. After a proper rescaling, the limit $\alpha \rightarrow \infty$ at fixed αD_0 yields purely potential velocity field. The exponent $0 < y < 2$ is a free parameter that might be interpreted as the Hölder exponent, which expresses a roughness of the velocity field. The Kolmogorov regime corresponds to the value $y = 4/3$, whereas the Batchelor limit (smooth velocity) is obtained in the limit $y \rightarrow 2$.

The action functional describing statistics of the velocity field \mathbf{v} is simply given by a quadratic form:

$$\mathcal{S}_{\text{vel}} = -\frac{1}{2} v_i D_{ij}^{-1} v_j, \quad (14)$$

where D_{ij}^{-1} is the kernel of the inverse linear operator in Eq. (13). This yields a propagator, Δ_{vv} , which in the time-momentum representation takes the following form:

$$\Delta_{vv}(t, \mathbf{k}) = w_0 \lambda_0 \delta(t) \frac{P_{ij}(\mathbf{k}) + \alpha Q_{ij}(\mathbf{k})}{k^{d+y}}. \quad (15)$$

For convenience, the factor D_0 from the kernel (13) has been expressed in the following way, $D_0 = \omega_0 \lambda_0$, so that RG constants might depend only on ω_0 .

To summarize, the total dynamic functional for model E with an inclusion of external velocity fluctuations is given by a sum of expressions (9) and (14), i.e.,

$$\mathcal{S} = \mathcal{S}_E + \mathcal{S}_{\text{vel}}. \quad (16)$$

Model (16) is amenable to the standard Feynman diagrammatic technique, which is based on the graphical interpretation of the linear (solvable) part of the action and the nonlinear terms therein [1,10]. In graphical means, interaction terms are represented by vertices, which are connected by lines. The latter correspond to propagators of the free theory, which are given by the quadratic part of the action. Propagators are conveniently given in the frequency-momentum representation:

$$\Delta_{mm} = \frac{2\lambda_0 u_0 k^2}{\omega^2 + \lambda_0^2 u_0^2 k^4} \theta(k - l_m), \quad (17)$$

$$\Delta_{mm'} = \frac{1}{-i\omega + \lambda_0 u_0 k^2}, \quad (18)$$

$$\Delta_{\psi'\psi^\dagger} = \Delta_{\psi'\psi} = \frac{1}{i\omega + \lambda_0 k^2}, \quad (19)$$

$$\Delta_{\psi\psi'} = \Delta_{\psi^\dagger\psi'} = \frac{1}{-i\omega + \lambda_0 k^2}, \quad (20)$$

$$\Delta_{\psi\psi^\dagger} = \Delta_{\psi^\dagger\psi} = \frac{2\lambda_0}{\omega^2 + \lambda_0^2 k^4} \theta(k - l_\psi), \quad (21)$$

where l_m and l_ψ are IR cutoff scales for fields m and ψ . For practical reasons we assume

$$l_v = l_m = l_\psi \equiv l \quad (22)$$

in actual evaluations of Feynman diagrams. This choice can be adopted because universal quantities do not depend on a particular choice of IR regularization [10,44].

With every interaction vertex, the algebraic factor

$$V_N(x_1, \dots, x_N; \varphi) = \frac{\delta^N \mathcal{S}[\varphi]}{\delta\varphi(x_1) \dots \delta\varphi(x_N)}$$

is associated [10], and φ is any field of the theory, i.e., $\varphi \in \Phi$, where

$$\Phi = \{\psi, \psi', \psi^\dagger, \psi'^\dagger, m, m', v\}. \quad (23)$$

Here, we readily find three vertex factors $V_{\psi'\psi^\dagger\psi\psi}$, $V_{\psi'\psi m}$, and $V_{m'\psi^\dagger\psi}$ plus their complex conjugates. Their explicit form can be easily inferred from action (9), and in the frequency-momentum representation, it explicitly reads

$$V_{\psi'\psi^\dagger\psi\psi} = -\frac{2g_{10}\lambda_0}{3}, \quad (24)$$

$$V_{\psi'\psi m} = -\lambda_0 g_{30}, \quad (25)$$

$$V_{m'\psi^\dagger(k)\psi(q)} = i\lambda_0 g_{30}[\mathbf{k}^2 - \mathbf{q}^2]. \quad (26)$$

The last vertex factor displays a nontrivial dependence on inflowing momenta of fields ψ^\dagger and ψ .

In addition, the set of propagators (17)–(19) has to be supplemented with the velocity propagator Δ_{vv} defined through

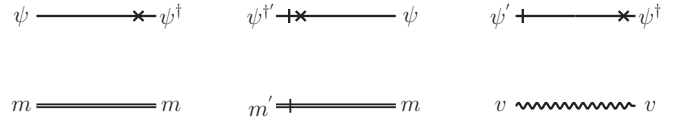


FIG. 1. A graphical representation of the free part of the action (16) that corresponds to lines in the Feynman diagrammatic technique.

the relations (12) and (13), respectively. Alternative interaction vertices arise from the convective terms (10) and (11) as well. Their vertex factors are

$$V_{\psi'\psi(k)v_i(q)} = V_{\psi'\psi^\dagger(k)v_i(q)} = ik_i + ia_{10}q_i, \quad (27)$$

$$V_{m'(k)v_i(q)} = ik_i + ia_{20}q_i. \quad (28)$$

Let us recall that the parameter y is not related to the spatial dimension and can be varied independently. For the RG analysis of the full-scale problem it is important that all the interactions become logarithmic simultaneously. Otherwise, one of them would be IR irrelevant with respect to the other and it should be discarded [10,44]. As a result, some of the scaling regimes of the full model would be lost. Instead of the ordinary ε expansion in the single-charge models, the coordinates of the fixed points, critical dimensions, and other quantities are now calculable in a double-expansion scheme (ε, y).

The perturbation theory of the model is amenable to the standard Feynman diagrammatic expansion [10,44,50]. A starting point of the perturbation theory is a free part of the action (16). By graphical means, it is represented as lines in the Feynman diagrams, whereas the nonlinear terms in Eq. (16) correspond to vertices connected by the lines. The bare propagators are graphically depicted in Fig. 1, and interaction vertices are depicted in Fig. 2.

III. RENORMALIZATION GROUP ANALYSIS

A standard goal in statistical physics lies in determination of the macroscopic (large-scale) behavior of the system. The RG procedure allows one to exploit scale invariance at the critical point and an elimination of UV divergences yields information about the IR behavior [10,44]. There are different prescriptions for the renormalization procedure.

In contrast to the usual situations in critical models, here we deal with a model exhibiting two small parameters, ε and y . Similarly, it has occurred in various contexts in the past [29,51,52]. Due to the presence of two formally small expansion parameters, the RG approach differs somewhat from a usual formalism. First, we assume that the model is regularized by means of an analytic regularization augmented with a dimensional regularization. As has been elucidated [53,54] the mostly used minimal subtraction (MS) scheme suffers from potential deficiencies and is thus not satisfactory from a theoretical point of view. Instead, for calculations of RG constants, we choose a normalization point scheme. Because we restrict ourselves here to the leading one-loop approximation, only two types of UV singularities arise: We find either a pole of type $1/\varepsilon$ or a pole of type $1/y$, respectively. Such a simple structure pertains only to the lowest orders in

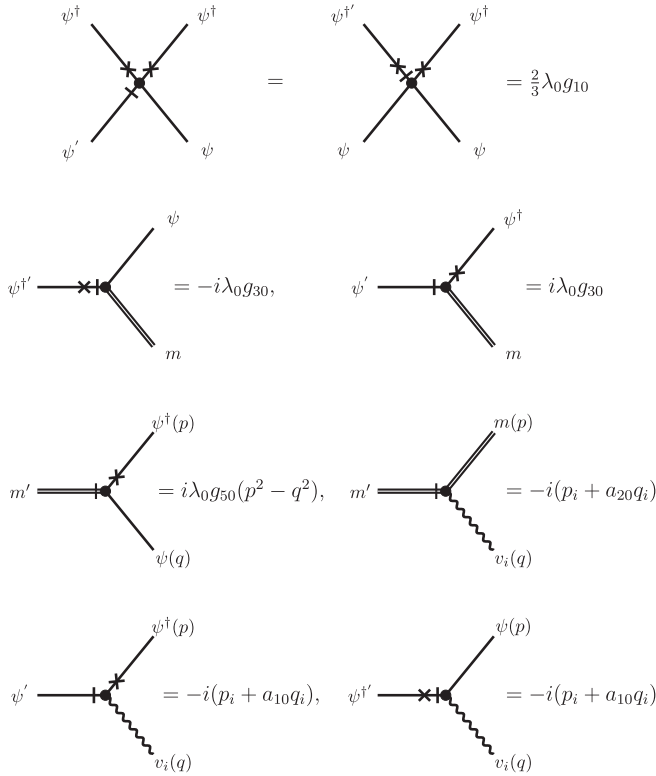


FIG. 2. A graphical representation of the nonlinear part of the action (16) that corresponds to interaction vertices in the Feynman diagrammatic technique.

a perturbation scheme. In higher loop-approximations, poles in the form of general linear combinations in ε and y are expected to arise. Moreover, nontrivial issues related to the vector character of fields are expected [55].

A. Canonical dimensions

A starting point of the RG approach is an analysis of canonical dimensions. Dynamical models of type (9), in contrast to static models, demonstrate two-scale behavior. This accounts for an assignment of two independent (momentum and frequency) canonical dimensions to each quantity F (a field or a parameter in the action functional). Further, since we work with the translationally invariant theory it is sufficient to analyze only one-particle-irreducible (1PI) functions of the model.

The momentum dimension d_F^k and the frequency dimension d_F^ω are determined from the standard normalization conditions,

$$\begin{aligned} d_k^k &= -d_x^k = 1, & d_\omega^k &= d_t^k = 0, \\ d_k^\omega &= d_x^\omega = 0, & d_\omega^\omega &= -d_t^\omega = 1, \end{aligned} \quad (29)$$

and from the requirement that each term in the action functional has to be a dimensionless quantity [10,44]. Then, based on d_F^k and d_F^ω one can introduce a total canonical dimension, $d_F = d_F^k + 2d_F^\omega$. (In the free theory, the time derivative ∂_t should scale in the same way as the Laplace operator ∂^2 .)

TABLE I. Canonical dimensions of the fields and parameters for model E with activated hydrodynamic modes defined by action (16).

Q	$p, 1/x$	$\omega, 1/t$	ψ, ψ^\dagger	ψ', ψ'^\dagger	m, m', h	v
d_Q^p	1	0	$\frac{d}{2} - 1$	$\frac{d}{2} + 1$	$\frac{d}{2}$	-1
d_Q^ω	0	1	0	0	0	1
d_Q	1	2	$\frac{d}{2} - 1$	$\frac{d}{2} + 1$	$\frac{d}{2}$	1
Q	λ_0	u_0	g_{10}	g_{30}, g_{50}	w_0	a_{10}, a_{20}, α
d_Q^p	-2	0	ε	$\frac{\varepsilon}{2}$	y	0
d_Q^ω	1	0	0	0	0	0
d_F	0	0	ε	$\frac{\varepsilon}{2}$	y	0

The dimensions of all quantities appearing in the action functional S are summarized in Table I. It follows that the model is logarithmic (the coupling constants become dimensionless) when $4 - d = 0$ ($\varepsilon = 0$) and $y = 0$. The total canonical dimension of an arbitrary 1PI function [10] is given by the relation

$$d_\Gamma = d + 2 - \sum_{\varphi \in \Phi} N_\varphi d_\varphi, \quad (30)$$

where the sum runs over a set of all fields Φ [defined in Eq. (23)] appearing in a given 1PI function Γ . The total dimension d_Γ is a formal index of the UV divergence. Due to the compressibility, the derivative ∂ on the external line m' in graphs of the 1PI functions cannot be singled out. It follows that the formal and real UV exponent are the same $d_\Gamma = \delta_\Gamma$. Superficial UV divergences, whose removal requires counterterms, can be present only in those functions Γ for which d_Γ is a non-negative integer [10]. It is easy to verify that all needed counterterms have a form of various terms already contained in action (9). By inspection of the graphs we observe that all nontrivial diagrams in the term $m' \partial_t m$ vanish. In Ref. [20] it has been demonstrated that the linkage to critical statics is violated due to the inclusion of the velocity field, but the multiplicative renormalization can be recovered by considering a new charge associated with the interaction term $m'(\psi^\dagger \nabla^2 \psi - \psi \nabla^2 \psi^\dagger)$. More precisely, instead of writing this term with the charge g_3 (see Eq. (5.149) in Chapter 5.20 in Ref. [10]), it has to be given as follows:

$$g_5 m'(\psi^\dagger \nabla^2 \psi - \psi \nabla^2 \psi^\dagger), \quad (31)$$

where, in general, a new charge g_5 does not coincide with the charge g_3 , i.e., $g_5 \neq g_3$. In summary, the field-theoretic renormalized action for model E with velocity fluctuations in condensed notation takes the following form:

$$\begin{aligned} \mathcal{S}_R &= 2Z_1 \lambda \psi'^\dagger \psi' - Z_2 \lambda u m' \partial^2 m' - \frac{1}{2} v D^{-1} v \\ &+ \psi'^\dagger \{-Z_3 \nabla_t \psi - Z_4 a_1 (\nabla \cdot \mathbf{v}) \psi + \lambda [Z_5 \partial^2 \psi \\ &- Z_6 g_1 \mu^\varepsilon (\psi^\dagger \psi) \psi / 3] + Z_7 i \lambda g_3 \mu^{\varepsilon/2} \psi [-m + h]\} \\ &+ \text{H.c.} + m' \{-Z_8 \nabla_t m - Z_9 a_2 (\nabla \cdot \mathbf{v}) m - \lambda u \partial^2 [-Z_{10} m \\ &+ h] + i \lambda g_5 \mu^{\varepsilon/2} Z_{11} [\psi^\dagger \partial^2 \psi - \psi \partial^2 \psi^\dagger]\}, \end{aligned} \quad (32)$$

where $\lambda, u, g_1, g_3, g_5, a_1$, and a_2 are renormalized analogs of the bare parameters (written with the subscript 0);

$Z_i, i = 1, \dots, 11$ are renormalization constants; and μ is the renormalization mass [10,44]. A full specification of employed normalization conditions reads as follows:

$$\Gamma_{\psi^+\psi'}|_* = 2\lambda, \quad (33)$$

$$\left. \frac{\partial \Gamma_{m'm'}}{\partial k^2} \right|_* = \lambda u, \quad (34)$$

$$\left. \frac{\partial \Gamma_{\psi^+\psi}}{\partial (i\Omega)} \right|_* = -\frac{1}{\lambda} \left. \frac{\partial \Gamma_{\psi^+\psi}}{\partial k^2} \right|_* = 1, \quad (35)$$

$$\left. \frac{\partial \Gamma_{m'm}}{\partial (i\Omega)} \right|_* = -\frac{1}{\lambda u} \left. \frac{\partial \Gamma_{m'm}}{\partial k^2} \right|_* = 1, \quad (36)$$

$$\Gamma_{\psi^+\psi m}|_* = -i\lambda g_3, \quad (37)$$

$$\left. \frac{\partial \Gamma_{m'\psi^+(\mathbf{p})\psi(\mathbf{q})}}{\partial \mathbf{p}^2} \right|_* = -\left. \frac{\partial \Gamma_{m'\psi^+(\mathbf{p})\psi(\mathbf{q})}}{\partial \mathbf{q}^2} \right|_* = i\lambda g_5, \quad (38)$$

$$\Gamma_{\psi^+\psi^+\psi\psi}|_* = -\frac{3\lambda g_1}{2}, \quad (39)$$

$$\left. \frac{\partial \Gamma_{\psi^+\psi(\mathbf{p})v_j(\mathbf{q})}}{\partial p_j} \right|_* = \frac{1}{a_1} \left. \frac{\partial \Gamma_{\psi^+\psi(\mathbf{p})v_j(\mathbf{q})}}{\partial q_j} \right|_* = -i, \quad (40)$$

$$\left. \frac{\partial \Gamma_{m'(\mathbf{p})v_j(\mathbf{q})}}{\partial p_j} \right|_* = \frac{1}{a_2} \left. \frac{\partial \Gamma_{m'(\mathbf{p})v_j(\mathbf{q})}}{\partial q_j} \right|_* = -i. \quad (41)$$

For convenience, we have introduced $*$ coordinates specified as follows:

$$\Omega_i = 0, \quad k_i = 0, \quad \mu = l, \quad (42)$$

where index i enumerates the independent external frequency or momenta entering given the 1PI function, and the IR scale l was introduced in Eq. (22).

The unrenormalized \mathcal{S} and the renormalized action functional \mathcal{S}_R are related by the standard formula

$$\mathcal{S}_R(\Phi) = \mathcal{S}(Z_\Phi \Phi).$$

Direct consequences of this formula are multiplicative relations for the fields $Z_\Phi \Phi = \{Z_\varphi \varphi : \varphi \in \Phi\}$ and parameters [10,44]

$$\begin{aligned} \lambda_0 &= \lambda Z_\lambda, & u_0 &= u Z_u, & g_{10} &= g_1 \mu^\varepsilon Z_{g_1}, \\ a_{10} &= a_1 Z_{a_1}, & a_{20} &= a_2 Z_{a_2}, & w_0 &= w \mu^\gamma Z_w, \\ g_{30} &= g_3 \mu^{\varepsilon/2} Z_{g_3}, & g_{50} &= g_5 \mu^{\varepsilon/2} Z_{g_5}. \end{aligned} \quad (43)$$

Since the term $\mathcal{S}_{\text{vel}}(\mathbf{v})$ given by Eq. (14) is nonlocal in the spatial variable, we know that according to general rules of the RG technique [10] it should not be renormalized. The parameter α is not renormalized at all, i.e., $\alpha_0 = \alpha$, and serves as a free parameter of the theory. Due to the Galilean symmetry ensured by the presence of the δ function in correlator (12), both terms in the Lagrangian derivative ∇_i are renormalized with the same renormalization constants. In addition, the quadratic term $v D^{-1} v / 2$ in the action (32) is not renormalized because of a passive nature of the advecting fields. As a direct consequence the velocity field \mathbf{v} is not renormalized and two

relations follow:

$$Z_w Z_\lambda = 1, \quad Z_\alpha = Z_v = 1. \quad (44)$$

In the leading one-loop approximation, the 1PI two-point Green's functions take the following forms:

$$\Gamma_{\psi^+\psi'} = 2\lambda Z_1 + \text{diagram 1} + \text{diagram 2}, \quad (45)$$

$$\Gamma_{m'm'} = \lambda u k^2 Z_2 + \text{diagram 3} + \text{diagram 4}, \quad (46)$$

$$\Gamma_{\psi^+\psi} = i\Omega Z_3 - \lambda k^2 Z_5 + \text{diagram 5} + \text{diagram 6}, \quad (47)$$

$$\Gamma_{m'm} = i\Omega Z_8 - \lambda u k^2 Z_{10} + \text{diagram 7} + \text{diagram 8}. \quad (48)$$

Let us note that, due to the structure of the vertex factors, the relation $Z_{m'} Z_m = 1$ is fulfilled.

Further, the 1PI Green's functions accounting for nonlinearities can be graphically represented as follows:

$$\Gamma_{\psi^+\psi m} = -i\lambda g_3 \mu^{\varepsilon/2} Z_7 + \text{diagram 9} + \text{diagram 10} + \text{diagram 11} + \text{diagram 12} + \text{diagram 13} + \text{diagram 14}, \quad (49)$$

$$\Gamma_{m'\psi^+(\mathbf{p})\psi(\mathbf{q})} = i\lambda g_5 \mu^{\varepsilon/2} (\mathbf{p}^2 - \mathbf{q}^2) Z_{11} + \text{diagram 15} + \text{diagram 16} + \text{diagram 17} + \text{diagram 18} + \text{diagram 19} + \text{diagram 20} + \text{diagram 21} + \text{diagram 22}, \quad (50)$$

$$\Gamma_{\psi+\psi+\psi+\psi} = -\frac{2}{3}\lambda g_1 \mu^\varepsilon Z_6 +$$

$$(51)$$

$$\Gamma_{\psi+\psi(\mathbf{p})v_j(\mathbf{q})} = -ip_j Z_3 - ia_1 q_j Z_4 +$$

$$(52)$$

$$\Gamma_{m' m(\mathbf{p})v_j(\mathbf{q})} = -ip_j Z_8 - ia_2 q_j Z_9 +$$

$$(53)$$

A major reduction of divergent diagrams comes from two observations. First, according to general rules of critical dynamics [10] any Feynman graph constructed solely from retarded propagators does not possess UV divergence. Second, a structure of interaction vertices allows one, in some cases, to pull out momentum dependence and thus reduce the effective dimension of internal momentum integration. This then also leads to UV convergence of the corresponding Feynman diagram.

A calculation in the employed RG scheme proceeds in a standard fashion and we have summarized all the results in Appendix A. Note that prefactors contain explicit d dependence stemming from the vector and tensorial character of interactions.

Technical difficulties related to the chosen IR cutoff were circumvented by a proper extraction of external momentum from a given diagram. Once the correct frequency or momentum dependence was pulled out of a diagram, it was permissible to set all external frequencies and momenta inside integrals to zero. This greatly simplifies calculations of divergent parts of Feynman diagrams. However, we expect this to be much more cumbersome in two- and higher-loop approximations.

B. RG functions

RG invariance [10,44] can be conveniently expressed by the differential equation $\mathcal{D}_\mu \Gamma = 0$, where the differentiation

with respect to renormalization mass μ in the operator $\mathcal{D}_\mu = \mu \partial_\mu$ is performed at fixed values of (bare) unrenormalized variables. For the 1PI renormalized Green's function, it can be rewritten as $[\mathcal{D}_{\text{RG}} - n_\Phi \gamma_\Phi] \Gamma_R(\mu, \dots) = 0$, where n_Φ is the number of fields of a given renormalized 1PI Green's function. The operator \mathcal{D}_{RG} stands for \mathcal{D}_μ in terms of the renormalized variables:

$$\mathcal{D}_{\text{RG}} \equiv \mu \frac{\partial}{\partial \mu} \Big|_0 = \mu \frac{\partial}{\partial \mu} + \sum_{g_i \in g} \beta_{g_i} \frac{\partial}{\partial g_i} - \gamma_\lambda \lambda \frac{\partial}{\partial \lambda}, \quad (54)$$

where the summation runs over all charges of the theory. For convenience we have introduced the compact notation

$$g \equiv \{g_1, g_3, g_5, u, w, a_1, a_2\}. \quad (55)$$

The differentiation in Eq. (54) at fixed values of the bare parameters is indicated explicitly by the subscript 0. The beta functions β_{g_i} and the anomalous dimensions γ_F of the mode are defined by the logarithmic derivatives [10,44]

$$\beta_i = \frac{\partial g_i}{\partial \ln \mu} \Big|_0, \quad \gamma_F = \frac{\partial \ln Z_F}{\partial \ln \mu} \Big|_0. \quad (56)$$

Straightforward application of these definitions to the relations (43) yields

$$\beta_{g_1} = g_1(-\varepsilon - \gamma_{g_1}), \quad \beta_{g_3} = g_3 \left(-\frac{\varepsilon}{2} - \gamma_{g_3} \right), \quad (57)$$

$$\beta_{g_5} = g_5 \left(-\frac{\varepsilon}{2} - \gamma_{g_5} \right), \quad \beta_w = w(-y - \gamma_w), \quad (58)$$

$$\beta_{a_1} = -a_1 \gamma_{a_1}, \quad \beta_{a_2} = -a_2 \gamma_{a_2}, \quad (59)$$

$$\beta_u = -u \gamma_u, \quad \beta_\alpha = -\alpha \gamma_\alpha. \quad (60)$$

In particular, the β_α function identically vanishes due to the aforementioned constraint $Z_\alpha = 1$. To obtain the remaining renormalization constants, the UV-divergent terms (poles in ε and y in our case) have to be extracted from the loop expansion of the corresponding 1PI functions. Renormalization constants Z_i , $i = 1, \dots, 11$, are related to the renormalization constants of the parameters and fields by means of the following relations:

$$Z_\lambda = Z_w^{-1} = \frac{Z_5}{Z_3}, \quad Z_u = \frac{Z_{10} Z_3}{Z_5 Z_8}, \quad (61)$$

$$Z_{g_5} = \frac{Z_{11} Z_1}{Z_5^2} \left(\frac{Z_{10}}{Z_2 Z_8} \right)^{1/2}, \quad Z_{g_1} = \frac{Z_6 Z_1}{Z_5^2 Z_3}, \quad (62)$$

$$Z_{g_3} = \frac{Z_7}{Z_5} \left(\frac{Z_2}{Z_{10} Z_8} \right)^{1/2}, \quad Z_{a_1} = \frac{Z_4}{Z_3}, \quad (63)$$

$$Z_{\psi'} = \left(\frac{Z_1 Z_3}{Z_5} \right)^{1/2}, \quad Z_\psi = \left(\frac{Z_3 Z_5}{Z_1} \right)^{1/2}, \quad (64)$$

$$Z_m = \left(\frac{Z_{10} Z_8}{Z_2} \right)^{1/2}, \quad Z_{a_2} = \frac{Z_9}{Z_8}, \quad (65)$$

$$Z_{m'} = \left(\frac{Z_2 Z_8}{Z_{10}} \right)^{1/2}, \quad (66)$$

where we have used two additional relations [10] for field renormalization:

$$Z_{\psi'} = Z_{\psi'^\dagger}, \quad Z_{\psi^\dagger} = Z_\psi. \quad (67)$$

From the second relation in (56) anomalous dimensions γ_F can be directly obtained from the renormalization constants (61)–(65). A special feature of the one-loop approximation is the fact that to this order we have found

$$Z_8 = Z_9 = 1. \quad (68)$$

Substituting Eq. (68) in Eq. (65) leads to

$$Z_{a_2} = 1. \quad (69)$$

Hence, parameter a_2 can be also regarded as a free parameter of the model to the order of perturbation theory.

IV. SCALING REGIMES AND THE FIXED-POINT STRUCTURE

From an experimental point of view, most relevant for statistical physics is the IR-asymptotic behavior, i.e., behavior of Green's functions at small frequencies $\omega \rightarrow 0$ and momenta $k \rightarrow 0$. This is related to large-scale macroscopic regimes of a given renormalizable field-theoretic model, which are associated with IR attractive fixed points of the corresponding RG equations [10,44]. A fixed point (FP) is defined as such a point $g^* \equiv \{g_1^*, g_3^*, g_5^*, u^*, a_1^*, a_2^*, w^*\}$ for which all β functions simultaneously vanish, i.e.,

$$\beta_{g_i}(g^*) = 0, \quad (70)$$

where g_i is any member of the set g defined in Eq. (55). The IR stability of a given fixed point is determined by the matrix of first derivatives of β functions:

$$\Omega_{ij} = \frac{\partial \beta_i}{\partial g_j} \Big|_{g^*}. \quad (71)$$

Coordinates of fixed points do not possess a direct physical information, because they depend on the chosen renormalization scheme [10,44]. However, in perturbation theory universal quantities and the number of fixed points actually depend on the chosen RG scheme [54]. In order to proceed in actual calculations, we have expanded prefactors containing the d parameter in Feynman diagrams by $d = 4 - \varepsilon$ (see Appendix A for details). Though not correct in higher-loop calculations, in the one-loop approximation this can be regarded as an adequate operation.

For completeness, we list all found fixed points in Appendix C.

For IR attractive fixed points all real parts of eigenvalues of matrix (71) are positive. Moreover, physical conditions $u^* > 0$ and $w^* > 0$ have to be fulfilled, which is due to their appearance in free pair correlation functions [see Eqs. (17) and (15)].

A thorough analysis of β functions has revealed that there are several possible regimes in cases without thermal fluctuations, i.e., regimes with a fixed-point coordinate $g_3^* = 0$. It is worth mentioning that for a purely transverse velocity field ($\alpha = 0$) the terms containing a_{10} and a_{20} in Eqs. (10) and (11) and all subsequent expressions vanish, and such parameters disappear from the model.

An actual analysis proved to be rather cumbersome and not very illuminating. The main technical problems were related to an appearance of parameters a_1 and a_2 brought about by compressibility of the velocity field in action (32). Moreover,

TABLE II. Intervals of free parameters a_1 , α , and a_2 with the corresponding inequality restricting the stability region of FP5. Here, α^* stands for the expression $3/(1 - 2a_1 - 2a_1^2)$.

a_1	α	a_2	Inequality
$(0, \frac{\sqrt{3}-1}{2})$	$(0, \alpha^*)$	$(0, \frac{4a_1^2-2a_1+1}{2a_1})$	(74)
$(0, \frac{\sqrt{3}-1}{2})$	$(0, \alpha^*)$	$(\frac{4a_1^2-2a_1+1}{2a_1}, \infty)$	(75)
$(0, \frac{\sqrt{3}-1}{2})$	(α^*, ∞)	$(0, \frac{3\alpha(2a_1^2-2a_1+1)-3}{4a_1\alpha})$	(73)
$(0, \frac{\sqrt{3}-1}{2})$	(α^*, ∞)	$(\frac{3\alpha(2a_1^2-2a_1+1)-3}{4a_1\alpha}, \infty)$	(75)
$(\frac{\sqrt{3}-1}{2}, \infty)$	$(0, \infty)$	$(0, \frac{4a_1^2-2a_1+1}{2a_1})$	(74)
$(\frac{\sqrt{3}-1}{2}, \infty)$	$(0, \infty)$	$(\frac{4a_1^2-2a_1+1}{2a_1}, \infty)$	(75)

the compressibility parameter α is free from any restriction and can attain any positive value [34]. Thus, when possible, we therefore try to present our findings by graphical means. Technical details can be found in the Appendixes.

Altogether eight fixed points have been found. However, only some of them are IR stable. A trivial Gaussian-like fixed point FP1 is IR stable in the region restricted by inequalities

$$\varepsilon < 0, \quad y < 0. \quad (72)$$

FP1 corresponds to a free model, for which all interactions are irrelevant, and is stable above the upper critical space dimension $d > d_c = 4$. The corresponding critical exponents attain their mean-field values.

The fixed points FP2, FP3, and FP4 are unstable because the corresponding eigenvalues of the Ω matrix (71) (see Table V) always contain one positive and one negative eigenvalue for any value of exponent ε .

For FP5 fixed points, values of charges g_1 , g_3 , and g_5 vanish identically. The nonzero coordinates w and u hint at the IR relevance of the turbulent advection. This regime corresponds to a well-known passive advection problem [24,34]. We recall that parameters α , a_1 , and a_2 should be regarded as free parameters and stability regions might exhibit a nontrivial dependence on them. This point is IR stable in the region restricted effectively by two inequalities. The first one is simply the condition $y > 0$, and the second restriction is given by one of the following inequalities:

$$[3 - \alpha(3a_1^2 - 3a_1 + 1)]y > \varepsilon \frac{3 + \alpha}{4}, \quad (73)$$

$$[3 - \alpha(8a_1^2 - 4a_1 + 1)]y > \varepsilon \frac{3 + \alpha}{2}, \quad (74)$$

$$[3 - \alpha(4a_1a_2 - 1)]y > \varepsilon \frac{3 + \alpha}{2}. \quad (75)$$

Which one of them will be imposed depends on the value of free parameters α , a_1 , and a_2 . The corresponding inequality for arbitrary value of parameters can be found in Table II. Parameter values corresponding to the endpoints in Table II lead to inequalities of the same form. A thorough analysis of FP5 reveals some interesting features. Increasing one of the free parameters with the two remaining parameters fixed, boundaries of the stability region shift. From a technical point of view, this is caused by a form of the left-hand side of

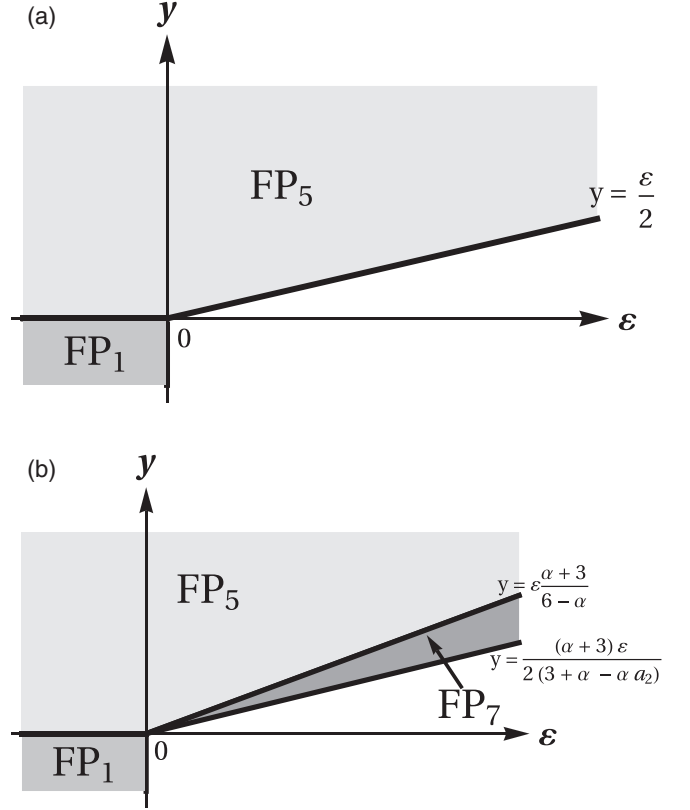


FIG. 3. Regions of stability of the fixed points in the model for the compressibility parameter $\alpha = 0$ (a) and for the following restricted choice of parameters $a_1 = 1/4$, $\alpha \in (0, \frac{8}{3})$, and $a_2 \in (0, \frac{3}{2})$ (b).

inequalities (73)–(75). For instance, we choose $a_1 = 1/4$ and a_2 from the interval $(0, \frac{3}{2})$. Then, whenever the compressibility parameter α attains a value smaller than $\alpha^* = 8$, the region of stability [Figs. 3(b), 4, and 5(a)] is restricted by inequality (74). On the other hand, for α larger than α^* , restrictions come from inequality (73). For a special case, $\alpha^* = 8$, the inequalities (73) and (74) are actually of the same form [Fig. 5(b)]. For $\alpha = 6$, the inequality (74) takes the simple form of $\varepsilon < 0$. With an increasing value of α , the boundary of FP5 rotates in the counterclockwise direction, and in the purely potential limit $\alpha \rightarrow \infty$ it approaches the ray $y = -\frac{4}{7}\varepsilon$. Let us note that in a one-loop approximation boundaries of stability regions between different fixed points are often given by straight lines. In a higher-loop calculation, overlapping regions might appear.

The remaining three regimes FP6, FP7, and FP8 are possible candidates for alternative regimes, since for them both velocity and self-interactions of model E are IR relevant. Fixed points FP5 and FP6 differ only in IR relevance of the self-interaction term $m'(\psi^\dagger \partial^2 \psi - \psi \partial^2 \psi^\dagger)$, which is irrelevant for the former and relevant for the latter. Similarly to the previous case of FP5, the stability region of FP6 is affected by values of free parameters a_1 , a_2 , and α . However, FP6 is realizable only for certain intervals, which can be summarized

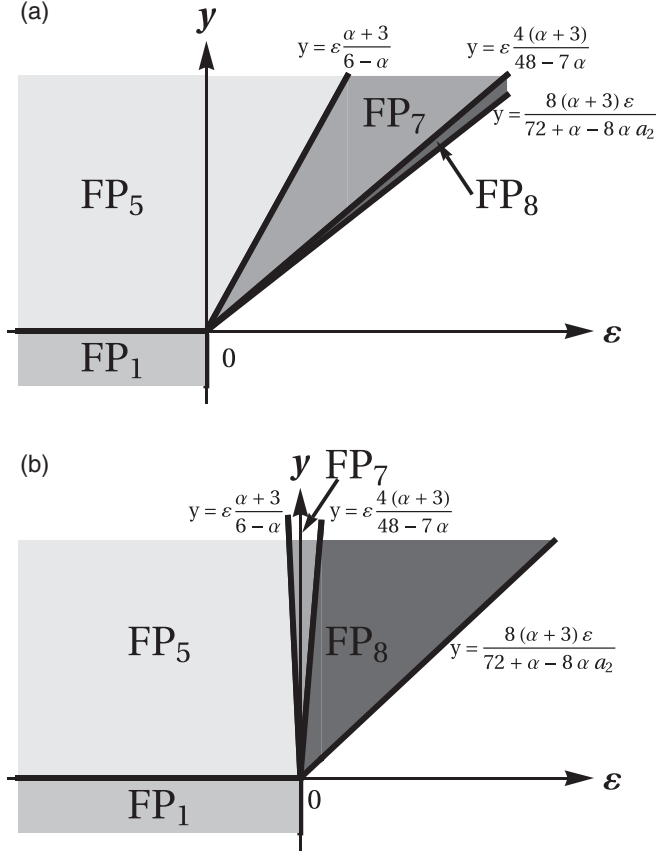


FIG. 4. Stability regions of the fixed points for which $a_1 = 1/4$ and for the following restricted choice of parameters $\alpha \in (\frac{8}{5}, 6)$ and $a_2 \in (0, \frac{15}{8} - \frac{3}{\alpha})$ (a) and $\alpha \in (6, \frac{48}{7})$ and $a_2 \in (0, \frac{15}{8} - \frac{3}{\alpha})$ (b).

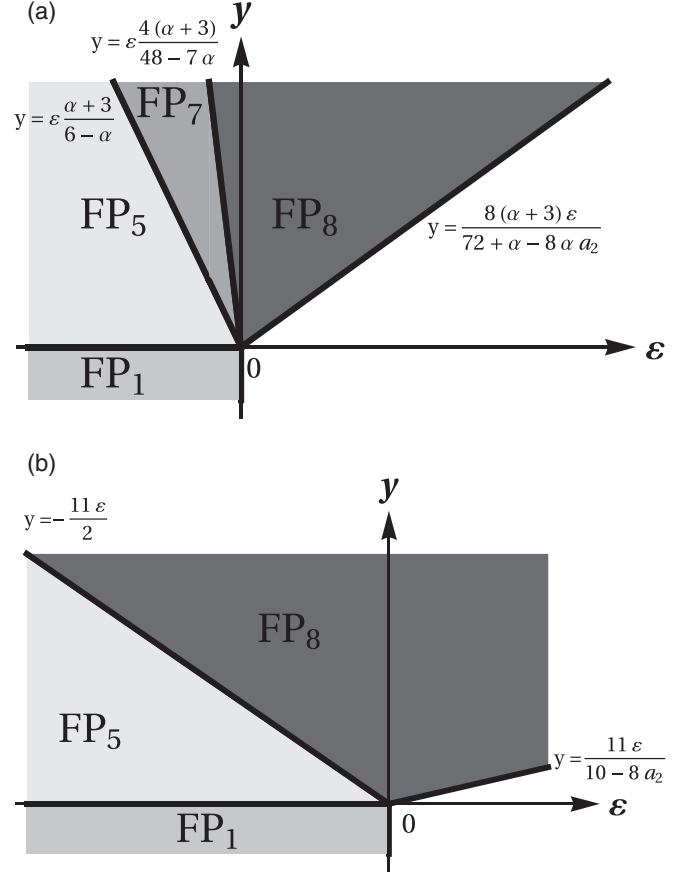


FIG. 5. Stability regions of the fixed points for which $a_1 = 1/4$ and for the following restricted choice of parameters $\alpha \in (\frac{48}{7}, 8)$ and $a_2 \in (0, \frac{1}{8} + \frac{9}{\alpha})$ (a) and $\alpha = 8$ and $a_2 \in (0, \frac{5}{4})$ (b).

as follows:

$$\begin{aligned} a_1 &\in \left(0, \frac{\sqrt{3}-1}{2}\right), \\ \alpha &\in \left(\frac{3}{1-2a_1-2a_1^2}, \infty\right), \\ a_2 &\in \left(0, \frac{3(\alpha-1)}{4a_1\alpha} + \frac{3(a_1-1)}{2}\right). \end{aligned} \quad (76)$$

The necessary condition for FP_6 being stable is $y > 0$. Further, it is restricted by the inverse inequality (73) as can be easily seen in Table V. The second restriction depends on the choice of the parameter a_2 . If the value of a_2 is smaller than the value $a_{2b} = (3+\alpha)/(4a_1\alpha) + (5a_1-1)/2$, the second boundary is given by the inequality (74). For $a_2 > a_{2b}$, the boundary is given by the following inequality:

$$[9 - \alpha(1 - 6a_1 + 6a_1^2 + 4a_1a_2)]y > \epsilon(3 + \alpha). \quad (77)$$

The overall analysis of FP_6 can be divided into two cases, whereby each of them corresponds to a different interval of parameters. The situation is qualitatively the same for $a_1 > 1/5$ as in the previous case of FP_5 . For $a_1 < 1/5$ the region

of stability lies in the first quadrant of the (ϵ, y) plane [see Fig. 6(b)].

For illustration purposes, the regions of IR stability in the (ϵ, y) plane are depicted in Fig. 6. The regime FP_6 is stable for the choice $a_1 = 1/4$, $\alpha > 8$, and the border is specified by Eq. (74) up to $a_2 = 9/8 + 3/\alpha$ [Fig. 6(a)]. With an increasing value of a_2 , the restriction changes to Eq. (77) and the stability region shrinks down into a boundary line for $a_2 = 15/8 - 3/\alpha$. Beyond the value $a_2 = 1 + 3/\alpha$, the border of FP_5 is specified by the inequality (75) and in the (ϵ, y) plane a void region appears between regimes FP_5 and FP_6 .

For the remaining two fixed points, FP_7 and FP_8 , the fixed points' coordinate of charge g_3 is zero. From the results in Appendix C it can be readily noticed that the main difference between regimes FP_5 and FP_7 lies in the IR relevance of the quartic interaction terms (proportional to the charge g_1). In addition, the coordinate a_1 attains a definite value of $1/4$ for the point FP_7 , whereas for FP_5 it is not fixed.

In contrast to a previously studied case, the stability analysis of FP_7 is less involved. First, one can show that the free parameters α and a_2 have to belong to the following intervals:

$$\alpha \in (0, 8), \quad a_2 \in (0, \frac{3}{2}). \quad (78)$$

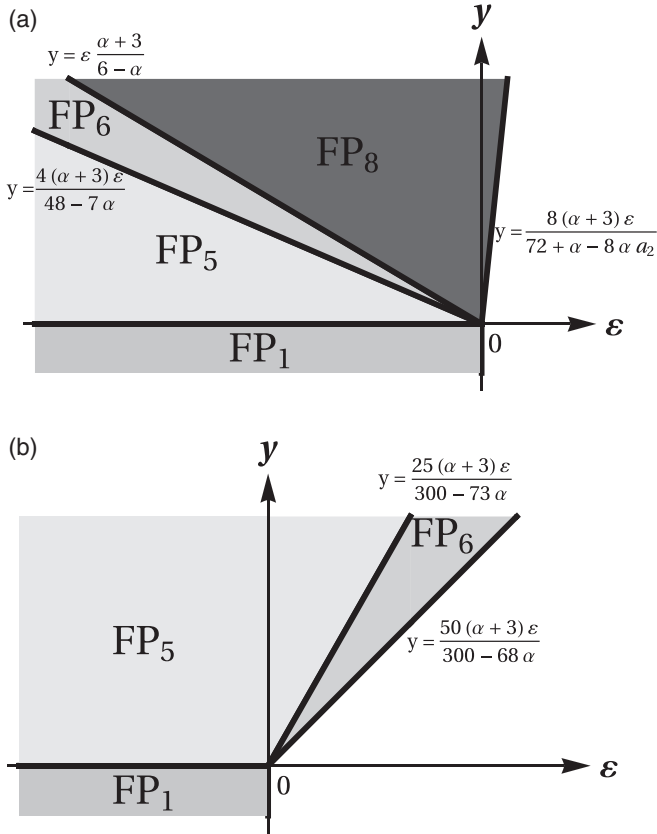


FIG. 6. Stability regions of the fixed points in the model for the following restricted choice of parameters $a_1 = 1/4$, $\alpha > 8$, and $a_2 \in (0, \frac{1}{8} + \frac{y}{\alpha})$ (a) and $a_1 = 1/10$, $\alpha \in (\frac{50}{13}, \frac{300}{73})$, and $a_2 \in (0, \frac{9}{4} + \frac{15}{2\alpha})$ (b).

Further, parameter y has to be strictly positive and further restrictions read as follows:

$$(3 + \alpha)\epsilon > (6 - \alpha)y, \quad (79)$$

$$(48 - 7\alpha)y > 4(3 + \alpha)\epsilon, \quad (80)$$

$$2[3 - \alpha(a_2 - 1)]y > (3 + \alpha)\epsilon. \quad (81)$$

For small values of the parameter a_2 the second restriction comes from Eq. (80) and it holds up to $a_2 = 15/8 - 3/\alpha$. Above this value, the boundary is defined by inequality (81).

Let us note that FP7 is unstable for the incompressible case [Fig. 3(a)], whereas even small (nonzero) values of α lead to its stabilization. With an increasing value of α , the region of IR stability rotates counterclockwise (see Fig. 4) and finally shrinks down to a boundary line $y = -11\epsilon/2$ for the limit value of compressibility parameter $\alpha = 8$ (see Fig. 5).

For the remaining fixed point FP8, parameters α and a_2 are restricted by the following conditions:

$$\alpha \in \left(\frac{8}{5}, \infty\right), \quad a_2 \in \left(0, \min\left\{\frac{9}{8} + \frac{3}{\alpha}, \frac{15}{8} - \frac{3}{\alpha}\right\}\right). \quad (82)$$

The stability region is always bounded by the inequality

$$[72 - \alpha(8a_2 - 1)]y > 8(3 + \alpha)\epsilon. \quad (83)$$

The second restriction is given by Eq. (80) with the opposite sign of inequality for $\alpha < 8$ and the regime is stable for $a_2 < 15/8 - 3/\alpha$. On the other hand, for $\alpha > 8$, the inequality (79) determines the boundary and FP8 is stable for $a_2 < 9/8 + 3/\alpha$. With an increasing value of the parameter α , the region of IR stability rotates counterclockwise. In the potential limit $\alpha \rightarrow \infty$ there always exists a stability region whenever $a_2 < 9/8$ is fulfilled. Once $a_2 > 9/8$, the regime becomes unstable.

It is worth mentioning that we have not found a nontrivial fixed point that would correspond to a case with all the nonlinearities being IR relevant. Notwithstanding this observation, activated velocity fluctuations affect the stability analysis through newly introduced charges g_5 , w , a_1 , and a_2 . From the practical point of view they contribute to the Ω matrix (71) with new columns and rows present.

Indeed, a comprehensive numerical analysis has revealed that they play an essential role in the fixed points' stability.

The same result has been obtained in the case of incompressible fluid [13]. We conclude that the presence of compressibility has a stabilizing effect on the regimes where nonlinearities are relevant. The regions of IR stability for these fixed points are shown in Figs. 3–6.

Let us focus on two special cases that correspond to the Kolmogorov spectrum of the velocity $y = 4/3$ and the Batchelor limit $y = 2$ (smooth velocity field), respectively. We can see that three fixed points belong to a given value of scaling parameter y for the real space dimension $d = 3$ ($\epsilon = 1$). The regime FP6 is located in a nonphysical region and could not be realized. Further, the analysis is focused on the case $a_1 = 1/4$, where the rest of the nontrivial regime is depicted in Fig. 7. For small values of the compressibility parameter α , both the Kolmogorov regime and the Batchelor limit belong to universality class FP5. As has been already mentioned, this regime corresponds to a passively advected scalar without self-interaction and for a small value of a_1 , a_2 , and α , it still can be stable for real scaling parameters y and ϵ . However, for a larger value of α , the Kolmogorov and Batchelor values happen to lie in the stability region (Fig. 7) of the alternative nontrivial regime FP7 or FP8.

Nevertheless, we expect that a qualitative picture for large values of compressibility should remain the same. In order to properly describe effects of strong compressibility and to better understand nonuniversal effects for turbulent mixing, one should proceed one step further and employ a more sophisticated model for compressible velocity fluctuations [52,56,57].

V. CRITICAL DIMENSIONS

The existence of an IR attractive fixed point implies the existence of scaling behavior of the Green's functions in the IR range. In this critical scaling all the IR irrelevant parameters (λ , μ , and the coupling constants) are fixed and the IR relevant parameters (coordinates/momenta, times/frequencies, and the fields) are dilated. In the leading IR asymptotic behavior of renormalized Green's functions G^R satisfy the RG equation (54) with the substitution $g \rightarrow g_*$ for the full set of the couplings [10,50]. This directly yields the fundamental

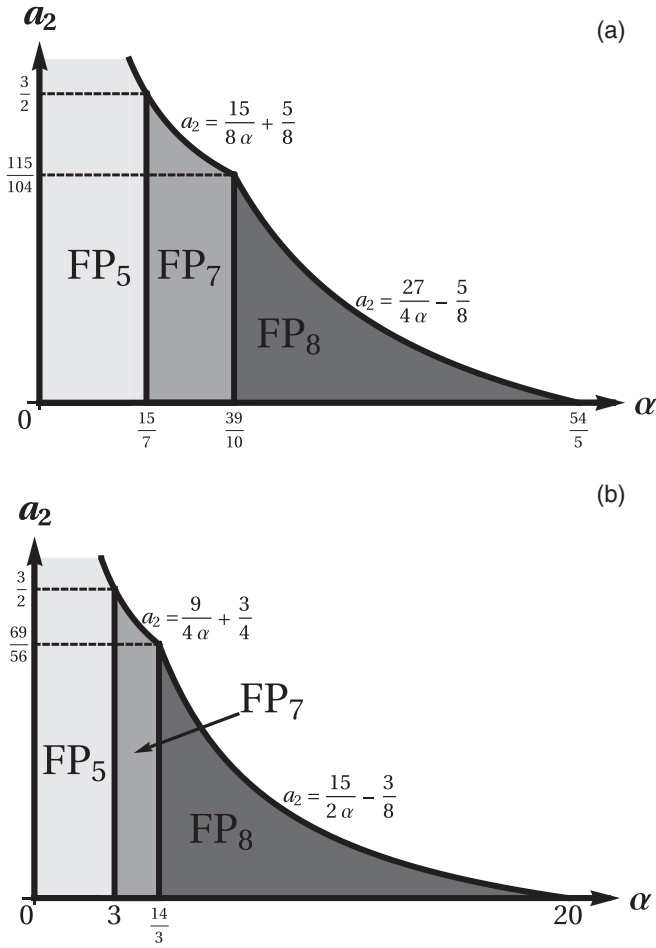


FIG. 7. Stability regions in the plane (α, a_2) in which depicted areas correspond to the fixed points for fixed parameters $\varepsilon = 1$ and $a_1 = 1/4$. Choice $y = 4/3$ corresponds to the Kolmogorov spectrum of velocity (a). Choice $y = 2$ corresponds to the Batchelor limit (b).

RG equation

$$\left\{ \mathcal{D}_\mu - \gamma_\lambda^* \mathcal{D}_\lambda + \sum_\varphi N_\varphi \gamma_\varphi^* \right\} G^R = 0, \quad (84)$$

where for convenience we write $\mathcal{D}_x \equiv x\partial/\partial x$, γ_F^* is the value of the anomalous dimension at the fixed point, and the summation over all types of the fields φ appearing in G^R is implied. Equations of this type describe the scaling with dilatation of the variables whose derivatives enter the differential operator [10,50].

The canonical scale invariance with respect to the momentum and frequency variable, respectively, can be expressed by two relations:

$$\left[\sum_\sigma d_\sigma^k \mathcal{D}_\sigma - d_G^k \right] G^R = 0, \quad \left[\sum_\sigma d_\sigma^\omega \mathcal{D}_\sigma - d_G^\omega \right] G^R = 0, \quad (85)$$

where σ is the full set of all the arguments of G^R , and d_σ^k and d_σ^ω are canonical dimensions of the variable σ with respect to momentum and frequency, respectively. In order to derive the proper scaling relation with fixed IR irrelevant parameters μ and ν , one has to combine Eqs. (84) and (85) in such

a way that the derivatives with respect to these parameters are eliminated [10,23]. This yields an equation of critical IR scaling for the model,

$$\left\{ -\mathcal{D}_x + \Delta_t \mathcal{D}_t + \Delta_\lambda \mathcal{D}_\lambda - \sum_\varphi N_\varphi \Delta_\varphi \right\} G^R = 0, \quad (86)$$

with the following notation

$$\Delta_F = d_F^k + \Delta_\omega d_F^\omega + \gamma_F^*, \quad \Delta_\omega = -\Delta_t = 2 - \gamma_\lambda^*. \quad (87)$$

Here, Δ_F is the critical dimension of the quantity F , while Δ_t and Δ_ω are the critical dimensions of time and frequency, and γ_F^* is the value of the anomalous dimension of a quantity F at the fixed point. In our case we have obtained critical dimensions for parameters and fields of IR stable fixed points in the following forms:

(i) FP1 (Gaussian fixed point)

$$\Delta_\omega = 2, \quad \Delta_\psi = \frac{d}{2} - 1, \quad \Delta_{\psi'} = \frac{d}{2} + 1, \quad (88)$$

$$\Delta_m = \Delta_{m'} = \frac{d}{2},$$

(ii) FP5 (passively advected scalar without self-interaction)

$$\begin{aligned} \Delta_\omega &= 2 - y, & \Delta_\psi &= 1 - \frac{\varepsilon}{2} + \frac{y}{2} - \frac{2\alpha y(a_1 - 1)^2}{3 + \alpha}, \\ \Delta_{\psi'} &= 3 - \frac{\varepsilon}{2} - \frac{y}{2} + \frac{2\alpha y(a_1 - 1)^2}{3 + \alpha}, \\ \Delta_m &= \Delta_{m'} = 2 - \frac{\varepsilon}{2}, \end{aligned} \quad (89)$$

(iii) FP6 (alternative nontrivial fixed point)

$$\begin{aligned} \Delta_\omega &= 2 - y, & \Delta_\psi &= 1 - \frac{\varepsilon}{2} + \frac{y}{2} - 2\alpha y \frac{(a_1 - 1)^2}{3 + \alpha}, \\ \Delta_{\psi'} &= 3 - \frac{\varepsilon}{2} - \frac{y}{2} + 2\alpha y \frac{(a_1 - 1)^2}{3 + \alpha}, \\ \Delta_m &= 2 - \varepsilon + 2y - \alpha y \frac{5 + 3(2a_1 - 1)^2}{2(3 + \alpha)}, \\ \Delta_{m'} &= 2 - 2y + \alpha y \frac{5 + 3(2a_1 - 1)^2}{2(3 + \alpha)}, \end{aligned} \quad (90)$$

(iv) FP7 (alternative nontrivial fixed point)

$$\begin{aligned} \Delta_\omega &= 2 - y, & \Delta_\psi &= 1 - \frac{\varepsilon}{2} + \frac{12 - 5\alpha}{8(3 + \alpha)} y, \\ \Delta_{\psi'} &= 3 - \frac{\varepsilon}{2} - \frac{12 - 5\alpha}{8(3 + \alpha)} y, \\ \Delta_m &= \Delta_{m'} = 2 - \frac{\varepsilon}{2}. \end{aligned} \quad (91)$$

(v) FP8 (alternative nontrivial fixed point)

$$\begin{aligned} \Delta_\omega &= 2 - y, & \Delta_\psi &= 1 - \frac{\varepsilon}{2} + \frac{12 - 5\alpha}{8(3 + \alpha)} y, \\ \Delta_{\psi'} &= 3 - \frac{\varepsilon}{2} - \frac{12 - 5\alpha}{8(3 + \alpha)} y, \\ \Delta_{m'} &= 2 - \frac{48 - 7\alpha}{8(3 + \alpha)} y, & \Delta_m &= 2 - \varepsilon + \frac{48 - 7\alpha}{8(3 + \alpha)} y. \end{aligned} \quad (92)$$

VI. CONCLUSION

We have incorporated effects of compressible turbulent mixing and stirring in model E of critical dynamics. It has been shown how the field-theoretic formulation of such a model can be constructed. A multiplicative renormalizability of the ensuing model has been proven, which permits us to employ a field-theoretic perturbative renormalization group. Altogether 62 nontrivial Feynman diagrams have been identified to the leading one-loop approximation. We have found that depending on the values of a spatial dimension ($d = 4 - \varepsilon$), a scaling exponent y describing statistics of velocity fluctuations, and a degree of compressibility α , the model exhibits 5 possible large-scale regimes corresponding to distinct universality classes. Two of them are already well-known: a Gaussian or trivial fixed point and a passively advected scalar without any self-interaction. The remaining three regimes correspond to alternative universality classes for which nonlinearities of model E and turbulent mixing are both relevant. Critical exponents have been calculated and they exhibit dependence on d and y and the compressibility parameter α . We have found that compressibility enhances the role of the nonlinear terms in the dynamical equations. The stability region in the (ε, y) plane, where alternative nontrivial regimes are stable, is thus getting much wider as the degree of compressibility increases. As a result, turbulent mixing becomes more efficient due to combined effects of the mixing and the nonlinear terms.

ACKNOWLEDGMENTS

The authors thank V. Škultéty for checking part of the calculations in Appendices A and B, and N. M. Gulitskiy for critical reading. The work was supported by VEGA Grant No. 1/0345/17 of the Ministry of Education, Science, Research and Sport of the Slovak Republic, and by the Slovak Research and Development Agency under Grant No. APVV-16-0186.

APPENDIX A: COMPUTATION OF FEYNMAN DIAGRAMS

In order to simplify notation we have used the following shift

of coupling constants:

$$\frac{eS_d}{(2\pi)^2} \rightarrow e, \quad (\text{A1})$$

where $S_d = 2\pi^{d/2}/\Gamma(d/2)$ is a convenient geometrical factor, and $e \in \{g_1, g_3^2, g_3g_5, g_5^2, w\}$. In order to avoid any potential ambiguities we explicitly indicate a symmetry coefficient of a given Feynman graph in front of its graphical representation. The assessment and direction of external momenta for 1PI diagrams $m'\psi\psi^\dagger$ correspond to independent momenta \mathbf{p} and \mathbf{q} displayed in Fig. 2. There, in vertex $\psi^\dagger\psi m'$, external momenta \mathbf{p} and \mathbf{q} flow in through fields $\psi^\dagger(\mathbf{p})$ and $\psi(\mathbf{q})$, and they flow out through $m'(-\mathbf{p}-\mathbf{q})$. The external momenta are chosen in such a way that they flow only via one internal line at most. Further, for 1PI diagrams $\psi^\dagger\psi v$, external momenta \mathbf{p} and \mathbf{q} flow in as $\psi(\mathbf{p})$ and $v_i(\mathbf{q})$ and then flow out as $\psi^\dagger(-\mathbf{p}-\mathbf{q})$, and finally, for diagrams $m'mv$, external

momenta \mathbf{p} and \mathbf{q} flow in as $m(\mathbf{p})$ and $v_i(\mathbf{q})$ and then flow out as $m'(-\mathbf{p}-\mathbf{q})$.

Let us also note that we give results only for diagrams that yield nonzero contributions:

$$\text{Diagram 1} = \frac{2\lambda g_3^2}{(1+u)\varepsilon}, \quad (\text{A2})$$

$$\text{Diagram 2} = \frac{\lambda(a_1-1)^2\alpha w}{y}, \quad (\text{A3})$$

$$\frac{1}{2} \text{Diagram 3} = \frac{2\lambda g_5^2 \mathbf{p}^2}{d\varepsilon}, \quad (\text{A4})$$

$$\frac{1}{2} \text{Diagram 4} = \frac{(d-1+\alpha)\lambda w \mathbf{p}^2}{2dy}, \quad (\text{A5})$$

$$\text{Diagram 5} = -\left[\frac{i\Omega}{(1+u)^2} + \lambda \mathbf{p}^2 \frac{4-d(u+1)}{d(1+u)^3} \right] \frac{g_3^2}{\varepsilon}, \quad (\text{A6})$$

$$\text{Diagram 6} = \frac{g_3g_5}{\varepsilon} \left[\frac{i\Omega}{(1+u)^2} - \lambda \mathbf{p}^2 \frac{(d(1+u)(2+u)-4)}{d(u+1)^3} \right], \quad (\text{A7})$$

$$\text{Diagram 7} = -\frac{\lambda(d-1+\alpha)w \mathbf{p}^2}{2dy}, \quad (\text{A8})$$

$$\text{Diagram 8} = -\frac{(d-2)\lambda g_3g_5 \mathbf{p}^2}{2d\varepsilon}, \quad (\text{A9})$$

$$\text{Diagram 9} = -\frac{(d-2)\lambda g_3g_5 \mathbf{p}^2}{2d\varepsilon}, \quad (\text{A10})$$

$$\text{Diagram 10} = \frac{(d-1+\alpha)\lambda w \mathbf{p}^2}{2dy}, \quad (\text{A11})$$

$$\text{Diagram 11} = -\frac{i\lambda g_1g_3}{3\varepsilon}, \quad (\text{A12})$$

$$\text{Diagram 12} = \frac{i\lambda g_1g_3}{3\varepsilon}, \quad (\text{A13})$$

$$\text{Diagram 13} = \frac{i\lambda g_3^3}{(1+u)^2\varepsilon}, \quad (\text{A14})$$

$$\text{Diagram 14} = \frac{-i\lambda(3+u)g_3^2g_5}{2(1+u)^2\varepsilon}, \quad (\text{A15})$$

$$\text{Diagram 15} = \frac{i\lambda g_3^2g_5}{2(1+u)\varepsilon}, \quad (\text{A16})$$

$$= -\frac{i\lambda g_3 \alpha a_1 a_2 w}{(1+u)y}, \quad (\text{A17})$$

$$= \frac{i\lambda g_5 g_1}{3d\varepsilon} \left[(6-d)\mathbf{p}^2 + (d-2)\mathbf{q}^2 + 4\mathbf{p} \cdot \mathbf{q} \right], \quad (\text{A18})$$

$$= -\frac{i\lambda g_5 g_1}{3d\varepsilon} \left[(6-d)\mathbf{p}^2 + (d-2)\mathbf{q}^2 + 4\mathbf{p} \cdot \mathbf{q} \right], \quad (\text{A19})$$

$$= i\lambda g_5 (\mathbf{p}^2 - \mathbf{q}^2) \frac{[d-4 + (d-2)u]g_3^2}{d(1+u)^2\varepsilon}, \quad (\text{A20})$$

$$= \frac{i\lambda g_5^2 g_3}{\varepsilon} \left[\frac{(6-d + (2-d)u)\mathbf{q}^2}{2d(1+u)^2} + \frac{(d-2)\mathbf{p}^2}{2d(1+u)} + \frac{4\mathbf{p} \cdot \mathbf{q}}{2d(1+u)^2} \right], \quad (\text{A21})$$

$$= -\frac{i\lambda g_5^2 g_3}{\varepsilon} \left[\frac{(d-2)\mathbf{q}^2}{2d(1+u)} + \frac{4\mathbf{p} \cdot \mathbf{q}}{2d(1+u)^2} + \frac{(6-d + (2-d)u)\mathbf{p}^2}{2d(1+u)^2} \right], \quad (\text{A22})$$

$$= (\mathbf{p}^2 - \mathbf{q}^2) \frac{i\lambda g_5 \alpha a_1 (2 + (d-2)a_1)w}{2dy}, \quad (\text{A23})$$

$$\frac{1}{2} = \frac{\lambda g_1^2}{9\varepsilon}, \quad (\text{A24})$$

$$= \frac{2\lambda g_1^2}{9\varepsilon}, \quad (\text{A25})$$

$$= \frac{2\lambda g_1^2}{9\varepsilon}, \quad (\text{A26})$$

$$\frac{1}{2} = \frac{\lambda g_1 g_3^2}{3(1+u)\varepsilon}, \quad (\text{A27})$$

$$= -\frac{2\lambda g_1 g_3^2}{3(1+u)\varepsilon}, \quad (\text{A28})$$

$$= \frac{2\lambda g_1 g_3^2}{3(1+u)^2\varepsilon}, \quad (\text{A29})$$

$$\frac{1}{2} = -\frac{\lambda g_1 g_3^2}{3(1+u)^2\varepsilon}, \quad (\text{A30})$$

$$= \frac{\lambda g_1 g_3 g_5}{3(1+u)\varepsilon}, \quad (\text{A31})$$

$$= -\frac{\lambda g_1 g_3 g_5}{3(1+u)\varepsilon}, \quad (\text{A32})$$

$$= \frac{\lambda g_1 g_3 g_5}{3(1+u)\varepsilon}, \quad (\text{A33})$$

$$\frac{1}{2} = \frac{\lambda(3+u)g_1 g_3 g_5}{6(1+u)^2\varepsilon}, \quad (\text{A34})$$

$$= -\frac{\lambda(3+u)g_1 g_3 g_5}{3(1+u)^2\varepsilon}, \quad (\text{A35})$$

$$= -\frac{\lambda g_1 g_3 g_5}{3(1+u)\varepsilon}, \quad (\text{A36})$$

$$\frac{1}{2} = \frac{\lambda g_1 g_3 g_5}{6(1+u)\varepsilon}, \quad (\text{A37})$$

$$= \frac{\lambda(1+2u)g_3^3g_5}{2u(1+u)^2\varepsilon}, \quad (\text{A38})$$

$$= \frac{\lambda(1+2u)g_3^3g_5}{2u(1+u)^2\varepsilon}, \quad (\text{A39})$$

$$= -\frac{\lambda(2+u)g_3^2g_5^2}{2u(1+u)^2\varepsilon}, \quad (\text{A40})$$

$$= -\frac{\lambda(2+u)g_3^2g_5^2}{2u(1+u)^2\varepsilon}, \quad (\text{A41})$$

$$= \frac{\lambda g_3^3g_5}{2u(1+u)^2\varepsilon}, \quad (\text{A42})$$

$$= \frac{\lambda g_3^3g_5}{2u(1+u)^2\varepsilon}, \quad (\text{A43})$$

$$= -\frac{\lambda g_3^2g_5^2}{2(1+u)^2\varepsilon}, \quad (\text{A44})$$

$$= -\frac{\lambda g_3^2g_5^2}{2(1+u)^2\varepsilon}, \quad (\text{A45})$$

$$= -\frac{\lambda g_1 \alpha a_1^2 w}{6y}, \quad (\text{A46})$$

$$= -\frac{\lambda g_1 \alpha a_1^2 w}{3y}, \quad (\text{A47})$$

$$= -\frac{\lambda \alpha a_1^2 w g_3 g_5}{2(1+u)y}, \quad (\text{A48})$$

$$= \frac{\lambda \alpha a_1^2 w g_3 g_5}{2(1+u)y}, \quad (\text{A49})$$

$$= -i q_1 \frac{1 - da_1}{3d\varepsilon} g_1, \quad (\text{A50})$$

$$= -i q_1 \frac{1 - da_1}{3d\varepsilon} g_1, \quad (\text{A51})$$

$$= i p_1 \frac{4u g_3^2}{d(1+u)^3\varepsilon} \quad (\text{A52})$$

$$- i q_1 \frac{[2 - d(1+u)a_1]g_3^2}{d(1+u)^3\varepsilon},$$

$$= -i p_1 \frac{u(5+u)g_3g_5}{d(1+u)^3\varepsilon} \quad (\text{A53})$$

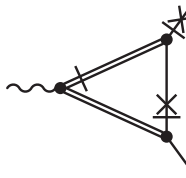
$$- \frac{i q_1 g_3 g_5}{2d(1+u)^3\varepsilon} [a_1 d(u^2 + 4u + 3) - (u^2 + 4u + 7)],$$

$$= i p_1 \frac{u g_3 g_5}{d(1+u)^2\varepsilon} - \frac{i q_1 g_3 g_5}{2d(1+u)^2\varepsilon} \quad (\text{A54})$$

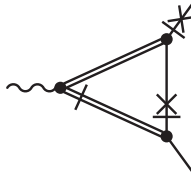
$$\times [5 + 3u + d(u+1)(a_1 - 1)],$$

$$= -i p_1 \frac{4g_3g_5}{d(1+u)^3\varepsilon} \quad (\text{A55})$$

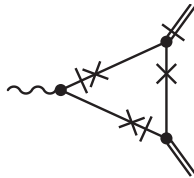
$$- i q_1 \frac{[-2u + d(1+u)a_2]g_3g_5}{d(1+u)^3\varepsilon},$$



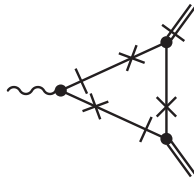
$$= ip_1 \frac{(1+5u)g_3^2}{du(1+u)^3\varepsilon} - \frac{iq_1g_3^2}{2du(1+u)^3\varepsilon} \times [1+4u+7u^2-d(1+4u+3u^2)a_2], \quad (\text{A56})$$



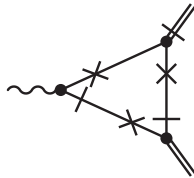
$$= iq_1 \frac{[1+3u+d(u+1)(a_2-1)]g_3^2}{2du(1+u)^2\varepsilon} - ip_1 \frac{g_3^2}{du(1+u)^2\varepsilon}, \quad (\text{A57})$$



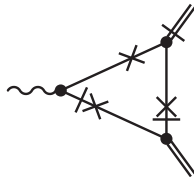
$$= ip_1 \frac{g_3g_5}{2d\varepsilon} + iq_1 \frac{g_3g_5}{2d\varepsilon}, \quad (\text{A58})$$



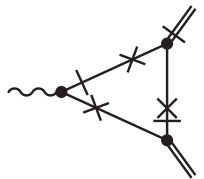
$$= ip_1 \frac{g_3g_5}{2d\varepsilon} + iq_1 \frac{g_3g_5}{2d\varepsilon}, \quad (\text{A59})$$



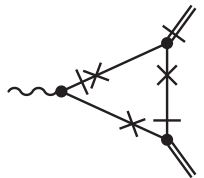
$$= ip_1 \frac{g_3g_5}{2d\varepsilon} + iq_1 \frac{g_3g_5}{2d\varepsilon}, \quad (\text{A60})$$



$$= ip_1 \frac{g_3g_5}{2d\varepsilon} + iq_1 \frac{g_3g_5}{2d\varepsilon}, \quad (\text{A61})$$



$$= -ip_1 \frac{g_3g_5}{d\varepsilon} - iq_1 \frac{g_3g_5}{d\varepsilon}, \quad (\text{A62})$$



$$= -ip_1 \frac{g_3g_5}{d\varepsilon} - iq_1 \frac{g_3g_5}{d\varepsilon}. \quad (\text{A63})$$

TABLE III. Coordinates of fixed points FP1 to FP6.

FP	FP1	FP2	FP3	FP4	FP5	FP6
g_1	0	$\frac{3\varepsilon}{5}$	0	$\frac{3}{5}\varepsilon$	0	0
g_3	0	0	$\sqrt{\varepsilon}$	$\sqrt{\varepsilon}$	0	0
g_5	0	0	$\sqrt{\varepsilon}$	$\sqrt{\varepsilon}$	0	$\sqrt{2\varepsilon + \frac{8[\alpha-3+3a_1\alpha(a_1-1)]}{\alpha+3}y}$
w	0	0	0	0	$\frac{8y}{3+\alpha}$	$\frac{8y}{3+\alpha}$
u	NF	NF	1	1	1	1
a_1	NF	$\frac{1}{4}$	$a_2 - \frac{1}{4}$	$5a_2 - \frac{9}{4}$	NF	NF

APPENDIX B: ANOMALOUS DIMENSIONS TO THE ONE-LOOP ORDER

In this section, we review the explicit expressions for the anomalous dimension γ_x , $x \in \{g_1, g_3, g_5, u, w, a_1, a_2\}$, of the charges and for the fields $x \in \{\psi, \psi', \mathbf{v}\}$, respectively. From relations (61)–(65), the following expressions directly follow:

$$\gamma_\lambda = -\gamma_w = \frac{4g_3^2}{d(1+u)^3} + \frac{g_3g_5[d-4+du(2+u)]}{d(1+u)^3} + \frac{w(d-1+\alpha)}{2d}, \quad (\text{B1})$$

$$\gamma_u = -\frac{4g_3^2}{d(1+u)^3} + \frac{w(d-1+\alpha)(1-u)}{2du} - \frac{g_3g_5[2u^3 - u^2(d-6) - 2u(d-1) + 2-d]}{du(1+u)^3}, \quad (\text{B2})$$

$$\gamma_{g_3} = -\frac{4g_3^2}{d(1+u)^3} + \frac{g_5^2}{du} - \frac{w}{2} \left(1 - \frac{1-\alpha}{d} - \frac{2a_1a_2\alpha}{1+u} \right) + \frac{g_3g_5[2(u^3+3u^2+7u+1) - d(1+u)^2(1+3u)]}{2du(1+u)^3}, \quad (\text{B3})$$

$$\gamma_{g_5} = \frac{2g_3^2[d(2+3u+u^2) - 6 - 3u - u^2]}{d(1+u)^3} + \frac{w}{d} \left[1 - d + \alpha \left(\frac{d-2}{2} + a_1(a_1-1)(d-1) \right) \right] + \frac{g_3g_5}{2du(1+u)^3} [2(u^3+3u^2+9u-1) - d(5u^3+13u^2+7u-1)] - \frac{g_5^2}{du}, \quad (\text{B4})$$

TABLE IV. Coordinates of fixed points FP7 and FP8.

FP	FP7	FP8
g_1	$\frac{3}{5}[\varepsilon + \frac{\alpha-6}{3+\alpha}y]$	$\frac{3}{5}[\varepsilon + \frac{\alpha-6}{3+\alpha}y]$
g_3	0	0
g_5	0	$\sqrt{2\varepsilon + \frac{7\alpha-48}{6+2\alpha}y}$
w	$\frac{8y}{3+\alpha}$	$\frac{8y}{3+\alpha}$
u	1	1
a_1	$\frac{1}{4}$	$\frac{1}{4}$

TABLE V. Eigenvalues of matrix Ω [see Eq. (71)] for IR-stable fixed points corresponding to regimes FP1 to FP5.

FP1	FP2	FP3	FP4	FP5
$-\varepsilon$	ε	$-\varepsilon$	$-\frac{\varepsilon}{10}$	$2y\frac{3-\alpha+3a_1\alpha(1-a_1)}{3+\alpha} - \frac{\varepsilon}{2}$
$-y$	$-\frac{\varepsilon}{2}$	$-\frac{\varepsilon}{2}$	$\frac{\varepsilon}{4}$	$2y\frac{3-\alpha+4a_1\alpha(1-2a_1)}{3+\alpha} - \varepsilon$
$-\frac{\varepsilon}{2}$	$-\frac{\varepsilon}{2}$	$\frac{\varepsilon}{4}$	ε	$y\frac{3+\alpha-4a_1a_2\alpha}{3+\alpha} - \frac{\varepsilon}{2}$
$-\frac{\varepsilon}{2}$	$\frac{2}{5}\varepsilon$	ε	ε	y
0	$-y$	$\frac{3\varepsilon}{2}$	$\frac{3\varepsilon}{2}$	y
0	0	$\frac{\varepsilon}{2} - y$	$\frac{\varepsilon}{2} - y$	0

TABLE VI. Eigenvalues of matrix Ω [see Eq. (71)] for IR-stable fixed points corresponding to regimes FP6 to FP8.

FP6	FP7	FP8
$\varepsilon + 4y\frac{\alpha-3+3a_1\alpha(a_1-1)}{3+\alpha}$	y	y
$2y\frac{3-\alpha+4a_1\alpha(1-2a_1)}{3+\alpha} - \varepsilon$	y	y
$\frac{9-\alpha+6a_1\alpha(1-a_1)-4a_1a_2\alpha}{3+\alpha} - \varepsilon$	$\frac{2}{5}(\varepsilon + y\frac{\alpha-6}{3+\alpha})$	$\frac{2}{5}(\varepsilon + y\frac{\alpha-6}{3+\alpha})$
y	$\varepsilon + y\frac{\alpha-6}{3+\alpha}$	$\varepsilon + y\frac{\alpha-6}{3+\alpha}$
y	$\frac{1}{8}(\frac{48-7\alpha}{3+\alpha}y - 4\varepsilon)$	$\frac{7\alpha-48}{4(3+\alpha)}y + \varepsilon$
0	$y - \frac{a_2y}{3+\alpha} - \frac{\varepsilon}{2}$	$y\frac{72+\alpha-8a_2\alpha}{8(3+\alpha)} - \varepsilon$

$$\gamma_{g_1} = \frac{2g_3[d(2+3u+u^2)-4](g_3-g_5)}{d(1+u)^3} - \frac{6g_3^2g_5(g_3-g_5)}{ug_1(1+u)} - \frac{5g_1}{3} + \frac{w}{d}\left[1-d+\alpha\left(\frac{d}{2}-1+da_1(2a_1-1)\right)\right], \quad (\text{B5})$$

$$\gamma_m = -\gamma_{m'} = \frac{g_3g_5(d-2)}{2du} - \frac{g_5^2}{du}, \quad (\text{B6})$$

$$\gamma_\psi = \gamma_{\psi'} = \frac{g_3(g_5-g_3)[d(3+4u+u^2)-4]}{2d(1+u)^3} + \frac{w}{4d}\{d-1-\alpha[d(a_1-1)^2-1]\}, \quad (\text{B7})$$

$$\gamma_{\psi'} = \gamma_{\psi''} = \frac{g_3(g_5-g_3)[4-d(1+u)^2]}{2d(1+u)^3} + \frac{w}{4d}\{1-d+\alpha[d(a_1-1)^2-1]\}, \quad (\text{B8})$$

$$\gamma_{a_1} = \frac{g_1(1-da_1)}{6a_1} + g_3g_5\frac{d(2+u)-4}{4(1+u)^2} + g_3^2\frac{4u(1+2a_1)+d[1+u-2a_1u-2a_2(1+2u)]}{8u(1+u)^2a_1} + \frac{g_3g_5}{8(1+u)^2a_1}\{d(2a_2-1-u)+2(u-1)+2a_1[d(2+u)-4]\}, \quad (\text{B9})$$

$$\gamma_{a_2} = 0. \quad (\text{B10})$$

APPENDIX C: COORDINATES OF FIXED POINTS

In this section, in Tables III and IV we list the coordinates of all fixed points for model E with compressible velocity fluctuations. The expression “not fixed” (NF) stands for a situation when a given fixed point coordinate cannot be unambiguously determined from a solution to RG flow equation (70).

The fixed point's value of the charge a_2 is in general not fixed; only for FP3 and FP4 is there an aforementioned relationship between a_1^* and a_2^* .

APPENDIX D: EIGENVALUES OF THE Ω MATRIX

In this section, in Tables V and VI, we list all the eigenvalues for the fixed points from Appendix C.

-
- [1] U. Täuber, *Critical Dynamics: A Field Theory Approach to Equilibrium and Non-Equilibrium Scaling Behavior* (Cambridge University, New York, 2014).
- [2] M. Henkel, H. Hinrichsen, and S. Lübeck, *Non-Equilibrium Phase Transitions: Volume 1: Absorbing Phase Transitions* (Springer, Dordrecht, 2008).
- [3] M. A. Muñoz, *Rev. Mod. Phys.* **90**, 031001 (2018).
- [4] D. ben-Avraham and S. Havlin, *Diffusion and Reactions in Fractals and Disordered Systems* (Cambridge University, Cambridge, England, 2000).
- [5] B. B. Mandelbrot, *Fractals and Scaling in Finance* (Springer, New York, 1997).
- [6] P. L. Krapivsky, S. Redner, and E. Ben-Naim, *A Kinetic View of Statistical Physics* (Cambridge University, Cambridge, England, 2010).
- [7] R. Pastor-Satorras, C. Castellano, P. Van Mieghem, and A. Vespignani, *Rev. Mod. Phys.* **87**, 925 (2015).
- [8] P. C. Hohenberg and B. I. Halperin, *Rev. Mod. Phys.* **49**, 435 (1977).
- [9] R. Folk and G. Moser, *J. Phys. A: Math. Gen.* **39**, R207 (2006).
- [10] A. N. Vasil'ev, *The Field Theoretic Renormalization Group in Critical Behavior Theory and Stochastic Dynamics* (CRC, Boca Raton, FL, 2004).

- [11] G. F. Mazenko, *Nonequilibrium Statistical Mechanics* (Wiley-VCH, Weinheim, 2006).
- [12] V. Dohm, *Phys. Rev. B* **73**, 092503 (2006).
- [13] M. Dančo, M. Hnatič, M. V. Komarova, T. Lučivjanský, and M. Yu. Nalimov, *Phys. Rev. E* **93**, 012109 (2016).
- [14] Y. A. Zhavoronkov, M. V. Komarova, Y. G. Molotkov, M. Y. Nalimov, and J. Honkonen, *Theor. Math. Phys.* **200**, 1237 (2019).
- [15] M. Hnatič, M. V. Komarova, and M. Y. Nalimov, *Theor. Math. Phys.* **175**, 779 (2013).
- [16] C. De Dominicis and L. Peliti, *Phys. Rev. Lett.* **38**, 505 (1977).
- [17] C. De Dominicis and L. Peliti, *Phys. Rev. B* **18**, 353 (1978).
- [18] V. Dohm, *Z. Phys. B* **33**, 79 (1979).
- [19] L. T. Adzhemyan, M. Dančo, M. Hnatič, E. V. Ivanova, and M. V. Kompaniets, *EPJ Web Conf.* **108**, 02004 (2016).
- [20] M. V. Komarova, D. M. Krasnov, and M. Y. Nalimov, *Theor. Math. Phys.* **169**, 1441 (2011).
- [21] M. Dančo, M. Hnatič, M. V. Komarova, D. M. Krasnov, T. Lučivjanský, L. Mižišin, and M. Y. Nalimov, *Theor. Math. Phys.* **176**, 888 (2013).
- [22] U. Frisch, *Turbulence: The Legacy of A. N. Kolmogorov* (Cambridge University, Cambridge, England, 1995).
- [23] L. T. Adzhemyan, N. V. Antonov, and A. N. Vasil'ev, *The Field Theoretic Renormalization Group in Fully Developed Turbulence* (Gordon & Breach, London, 1999).
- [24] G. Falkovich, K. Gawędzki, and M. Vergassola, *Rev. Mod. Phys.* **73**, 913 (2001).
- [25] D. Y. Ivanov, *Critical Behavior of Non-Idealized Systems* (Fizmatlit, Moscow, 2003).
- [26] D. E. Khmel'nitski, *Zh. Eksp. Teor. Fiz.* **68**, 19 (1975) [*Sov. Phys. JETP* **41**, 981 (1975)].
- [27] H. K. Janssen, K. Oerding, and E. Sengespeick, *J. Phys. A: Math. Gen.* **28**, 6073 (1995).
- [28] G. Satten and D. Ronis, *Phys. Rev. Lett.* **55**, 91 (1985).
- [29] G. Satten and D. Ronis, *Phys. Rev. A* **33**, 3415 (1986).
- [30] N. V. Antonov, *J. Phys. A: Math. Gen* **39**, 7825 (2006).
- [31] R. H. Kraichnan, *Phys. Fluids* **11**, 945 (1968).
- [32] N. V. Antonov, *Phys. Rev. E* **60**, 6691 (1999).
- [33] L. T. Adzhemyan, N. V. Antonov, and J. Honkonen, *Phys. Rev. E* **66**, 036313 (2002).
- [34] N. V. Antonov, *Phys. D (Amsterdam, Neth.)* **144**, 370 (2000).
- [35] N. V. Antonov, M. Hnatič, J. Honkonen, and M. Jurcisin, *Phys. Rev. E* **68**, 046306 (2003).
- [36] M. Chertkov, G. Falkovich, and V. Lebedev, *Phys. Rev. Lett.* **76**, 3707 (1996).
- [37] G. Eyink, *Phys. Rev. E* **54**, 1497 (1996).
- [38] M. Vergassola and M. Avellaneda, *Phys. D (Amsterdam, Neth.)* **106**, 148 (1997).
- [39] L. T. Adzhemyan and N. V. Antonov, *Phys. Rev. E* **58**, 7381 (1998).
- [40] J. Honkonen, *Theor. Math. Phys.* **175**, 827 (2013).
- [41] J. Honkonen, M. V. Komarova, Y. G. Molotkov, and M. Y. Nalimov, *Nucl. Phys. B* **939**, 105 (2019).
- [42] A. N. Vasil'ev, *Functional Methods in Quantum Field Theory and Statistical Physics* (CRC, Boca Raton, FL, 1998).
- [43] L. D. Landau and E. M. Lifshitz, *Fluid Mechanics* (Pergamon, Elmsford, NY, 1959).
- [44] J. Zinn-Justin, *Quantum Field Theory and Critical Phenomena*, 4th ed. (Oxford University, Oxford, 2002).
- [45] H. K. Janssen, *Z. Phys. B* **23**, 377 (1976).
- [46] C. D. Dominicis, *J. Phys. (Paris)* **37**, C1-247 (1976).
- [47] P. C. Martin, E. D. Siggia, and H. A. Rose, *Phys. Rev. A* **8**, 423 (1973).
- [48] N. V. Antonov and A. S. Kapustin, *J. Phys. A: Math. Theor.* **43**, 405001 (2010).
- [49] K. Gawędzki and M. Vergassola, *Phys. D (Amsterdam, Neth.)* **138**, 63 (2000).
- [50] D. J. Amit and V. Martín-Mayor, *Field Theory, the Renormalization Group, and Critical Phenomena* (World Scientific, Singapore, 2005).
- [51] A. Weinrib and B. I. Halperin, *Phys. Rev. B* **27**, 413 (1983).
- [52] D. Y. Volchenkov and M. Y. Nalimov, *Theor. Math. Phys.* **106**, 307 (1996).
- [53] L. T. Adzhemyan, M. Hnatič, and J. Honkonen, *Eur. Phys. J. B* **73**, 275 (2010).
- [54] J. Honkonen, *Chaotic modeling and simulation (CMSIM)* **2**, 139 (2018).
- [55] K. J. Wiese, *Phys. Rev. E* **56**, 5013 (1997).
- [56] N. V. Antonov, M. Yu. Nalimov, and A. A. Udalov, *Theor. Math. Phys.* **110**, 305 (1997).
- [57] N. V. Antonov, N. M. Gulitskiy, M. M. Kostenko, and T. Lučivjanský, *Phys. Rev. E* **95**, 033120 (2017).